show that 9 out of 10 kits tested are capable of detecting as low as 0.2 IU/ml HBsAg including HBV genotypes F and H, alleviating this concern.

Acknowledgments

We are grateful to the manufacturers who kindly supplied us with the HBsAg diagnostic kits and helped us in performing the assays.

References

Arauz-Ruiz, P., Norder, H., Robertson, B.H., Magnius, L.O., 2002. Genotype H: a new Amerindian genotype of hepatitis B virus revealed in Central America. J. Gen. Virol. 83, 2059–2073.

Chu, C.J., Hussain, M., Lok, A.S., 2002. Hepatitis B virus genotype B is associated with earlier HBeAg seroconversion compared with hepatitis B virus genotype C. Gastroenterology 122, 1756–1762.

Günther, S., Li, B.-C., Miska, S., Kruger, D.H., Meisel, H., Will, H., 1995. A novel method for efficient amplification of whole hepatitis B virus genomes permits rapid functional analysis and reveals deletion mutants in immunosuppressed patients. J. Virol. 69, 5437–5444.

Ishikawa, K., Koyama, T., Masuda, T., 2002. Prevalence of HBV genotypes in asymptomatic carrier residents and their clinical characteristics during long-term follow-up: the relevance to changes in the HBeAg/anti-HBe system. Hepatol. Res. 24, 1–7.

Kao, J.H., Chen, P.J., Lai, M.Y., Chen, D.S., 2000a. Hepatitis B genotypes correlate with clinical outcomes in patients with chronic hepatitis B. Gastroenterology 118, 554–559.

Kao, J.H., Wu, N.H., Chen, P.J., Lai, M.Y., Chen, D.S., 2000b. Hepatitis B genotypes and the response to interferon therapy. J. Hepatol. 33, 998–1002.

Kao, J.H., Liu, C.J., Chen, D.S., 2002. Hepatitis B viral genotypes and lamivudine resistance. J. Hepatol. 36, 303–304.

Mayerat, C., Mantgegani, A., Frei, P.C., 1999. Does hepatitis B virus (HBV) genotype influence the clinical outcome of HBV infection? J. Viral Hepat. 6, 299–304.

Mizuochi, T., Okada, Y., Umemori, K., Mizusawa, S., Sato, S., Yamaguchi, K., 2005. Reactivity of genotypically distinct hepatitis B virus surface antigens in 10 commercial diagnostic kits available in Japan. Jpn. J. Inf. Dis. 58, 83–87.

Nakabayashi, H., Taketa, K., Miyano, K., Yamane, T., Sato, J., 1982. Growth of human hepatoma cells lines with differentiated functions in chemically defined medium. Cancer Res. 42, 3858–3863.

Norder, H., Courouce, A.M., Magnius, L.O., 1994. Complete genomes, phylogenetic relatedness, and structural proteins of six strains of the hepatitis B virus, four of which represent two new genotypes. Virology 198, 489–503.

Norder, H., Courouce, A.-M., Coursaget, P., Echevarria, J.M., Lee, S.-D., Mushahwar, I.K., Robertson, B.H., Locarnini, S., Magnius, L.O., 2004. Genetic diversity of hepatitis B virus strains derived worldwide: genotypes, subgenotypes, and HBsAg subtypes. Intervirology 47, 289–309.

Okamoto, H., Tsuda, F., Sakugawa, H., Sastrosoewignjo, R.I., Imai, M., Miyakawa, Y., Mayumi, M., 1988. Typing hepatitis B virus by homology in nucleotide sequence: comparison of surface antigen subtypes. J. Gen. Virol. 69, 2575–2583.

Orito, E., Mizokami, M., 2003. Hepatitis B virus genotypes and hepatocellular carcinoma in Japan. Intervirology 46, 408–412.

Stuyver, L., De Gendt, S., Van Geyt, C., Zoulim, F., Fried, M., Schinazi, R.F., Rossau, R., 2000. A new genotype of hepatitis B virus: complete genome and phylogenetic relatedness. J. Gen. Virol. 81, 67–74.

Wai, C.T., Chu, C.J., Hussain, M., Lok, A.S., 2002. HBV genotype B is associated with better response to interferon therapy in HBeAg(+) chronic hepatitis than genotype C. Hepatology 36, 1425–1430.

Zollner, B., Petersen, J., Puchhammer-Stockl, E., Kletzmayr, J., Sterneck, M., Fischer, L., Schroeter, R., Feucht, H.H., 2004. Viral features of lamivudine resistant hepatitis B genotypes A and D. Hepatology 39, 42–50.

Available online at www.sciencedirect.com
SCIENCE DIRECT
ELSEVIER
Virology 345 (2006) 434 – 445
VIROLOGY
www.elsevier.com/locate/yviro

Down-regulation of the internal ribosome entry site (IRES)-mediated translation of the hepatitis C virus: Critical role of binding of the stem-loop IIId domain of IRES and the viral core protein

Takashi Shimoike [a,*], Chika Koyama [a], Kyoko Murakami [b], Ryosuke Suzuki [b], Yoshiharu Matsuura [c], Tatsuo Miyamura [a,b], Tetsuro Suzuki [b,*]

[a] *Department of Virology II, National Institute of Infectious Diseases, Musashi-murayama, Tokyo 208-0011, Japan*
[b] *Department of Virology II, National Institute of Infectious Diseases, Shinjuku-ku, Tokyo 162-8640, Japan*
[c] *Research Center for Emerging Infectious Diseases, Research Institute for Microbial Diseases, Osaka University, Suita-shi, Osaka 565-0871, Japan*

Received 27 May 2005; returned to author for revision 1 July 2005; accepted 7 October 2005
Available online 17 November 2005

Abstract

In a previous study, we observed that hepatitis C virus (HCV) core protein specifically inhibits translation initiated by an HCV internal ribosome entry site (IRES). To investigate the mechanism by which down-regulation of HCV translation occurs, a series of mutations were introduced into the IRES element, as well as the core protein, and their effect on IRES activity examined in this study. We found that expression of the core protein inhibits HCV translation possibly by binding to a stem-loop IIId domain, particularly a GGG triplet within the hairpin loop structure of the domain, within the IRES. Basic-residue clusters located at the N-terminus of the core protein have an inhibitory effect on HCV translation, and at least one of three known clusters is required for inhibition. We propose a model in which competitive binding of the core protein for the IRES and 40S ribosomal subunit regulates HCV translation.

Keywords: Hepatitis C virus; Internal ribosome entry site; Translation; Core protein

Introduction

Hepatitis C virus (HCV) is a major causative agent of chronic hepatitis, liver cirrhosis, and hepatocellular carcinoma (Alter and Seeff, 2000; Pawlotsky, 2004). HCV contains approximately 9.6 kb of positive-strand RNA with one open reading frame encoding a precursor polyprotein, which is proteolytically cleaved to produce the mature structural and non-structural proteins of HCV (Choo et al., 1991; Grakoui et al., 1993; Hijikata et al., 1991; Takamizawa et al., 1991). Although HCV exhibits considerable genetic diversity, the 5′ untranslated region (5′UTR) of the viral genome is relatively well conserved among all genotypes.

HCV translation is initiated by a cap-independent mechanism involving an internal ribosome entry site (IRES), comprising nearly the entire 5′UTR of the genome. There is evidence to suggest that the first 12 to 30 nucleotides (nt) of the coding sequence are also important for IRES activity (Hellen and Pestova, 1999; Lu and Wimmer, 1996; Reynolds et al., 1995). The proposed secondary structure of the HCV 5′UTR, thought to contain four major domains (I to IV) (Fig. 1), may be conserved among HCV and related flaviviruses and pestiviruses (Brown et al., 1992; Honda et al., 1999a, 1999b; Zhao and Wimmer, 2001).

Recruitment of the 43S ribosomal complex, containing a small 40S ribosomal subunit, eukaryotic initiation factor (eIF) 3, and a tRNA–eIF2–GTP ternary complex, to mRNA molecules is critical for initiation of eukaryotic protein synthesis. The 40S subunit and eIF3 can bind independently to the HCV IRES (Buratti et al., 1998; Hellen and Pestova, 1999; Kieft et al., 2001; Sizova et al., 1998). However, it appears that interaction between IRES RNA and the 40S

* Corresponding authors. T. Shimoike is to be contacted at fax: +81 42 561 4729. T. Suzuki, fax: +81 3 5285 1161.
E-mail addresses: shimoike@nih.go.jp (T. Shimoike), tesuzuki@nih.gi.jp (T. Suzuki).

0042-6822/$ - see front matter © 2005 Elsevier Inc. All rights reserved.
doi:10.1016/j.virol.2005.10.013

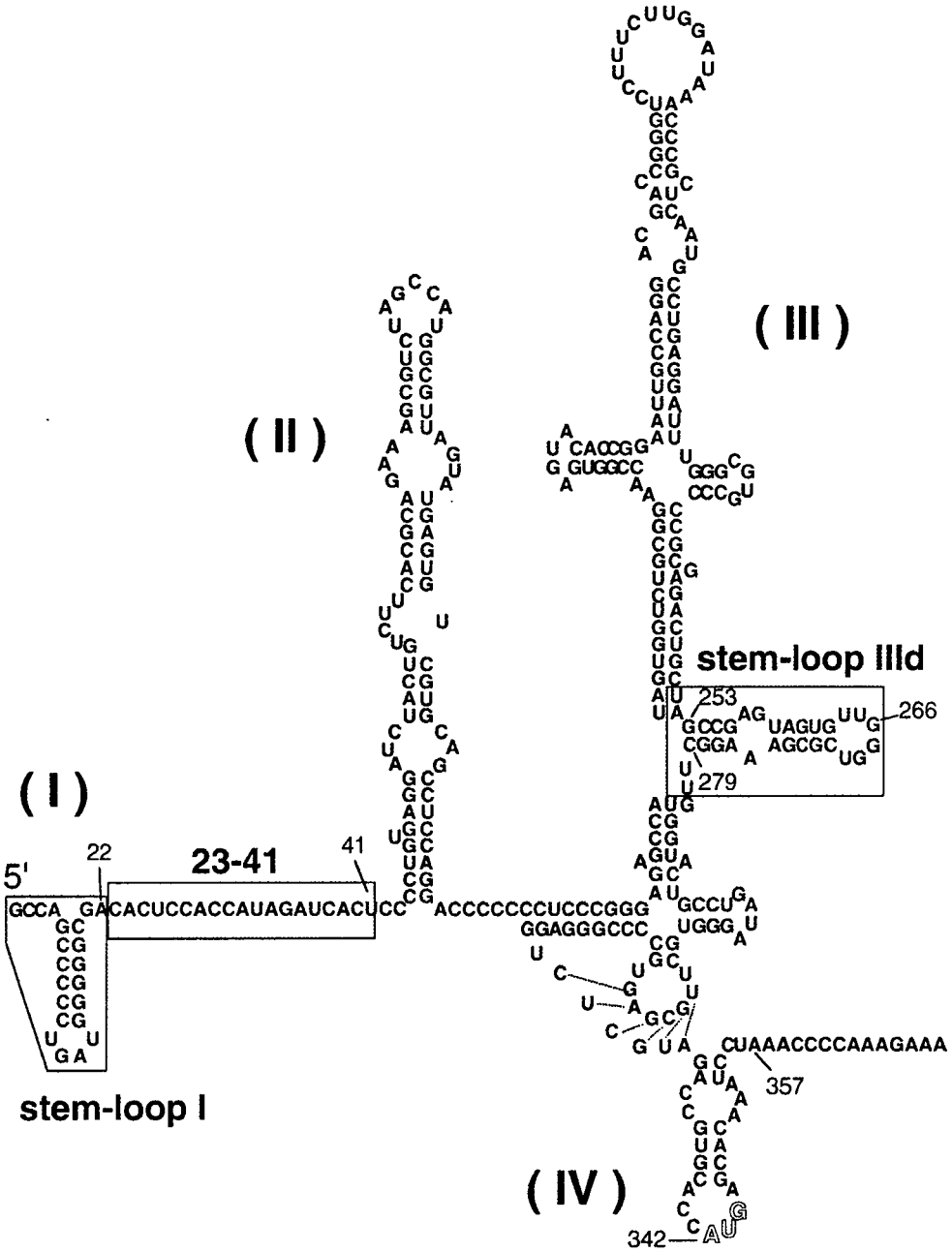

Fig. 1. Predicted secondary structure of the HCV 5′UTR (Honda et al., 1999a, 1999b). The stem-loop I, nt 23–41, and stem-loop IIId domains are highlighted. The initiator AUG codon is shown in the sequence of loop IV. Small numerals indicate the nucleotide positions from the 5′end.

subunit drives formation of the IRES-40S subunit–eIF3 complex since HCV IRES RNA demonstrates similar affinity for the 40S subunit and the 40S–eIF complex (Kieft et al., 2001). Other cellular factors such as La autoantigen (Ali et al., 2000; Ali and Siddiqui, 1997; Isoyama et al., 1999), heterogeneous ribonucleoprotein L (Hahm et al., 1998), poly-C binding protein (Fukushi et al., 2001; Spangberg and Schwartz, 1999), and pyrimidine tract-binding protein (Ali and Siddiqui, 1995; Anwar et al., 2000) also bind to the IRES element and modulate translation.

HCV core protein, which is located at the N-terminus of the viral polyprotein, is a putative nucleocapsid protein given the basic nature of its amino acid (aa) residues and the organization of the HCV genome. HCV core protein can form multimeric complexes, as well as heterodimer complexes with envelope E1 protein (Lo et al., 1996). Physical interaction between the core protein and viral genomic RNA is thought to occur during nucleocapsid formation. The results of several Northwestern analyses suggest that the core protein binds to the 5′UTR of the HCV genome, regardless of the specific RNA sequences involved (Santolini et al., 1994; Hwang et al., 1995; Fan et al., 1999). We previously used both in vivo and in vitro systems to demonstrate that the core protein preferentially binds to positive-stranded viral RNA containing the 5′UTR and

part of the structural protein-coding region (Shimoike et al., 1999). In addition, the core protein has a high affinity for the stem-loop IIId domain of the 5′UTR (Fig. 1) and for (G)-rich nucleotides (Tanaka et al., 2000).

In addition, evidence regarding the importance of the interaction between HCV core protein and HCV RNA in regulating viral translation is accumulating. We previously reported that expression of the core protein down-regulates HCV translation through interaction(s) involving 5′ regions of the viral genome (Shimoike et al., 1999). Although some evidence suggesting inhibition of HCV translation through RNA–RNA interactions, rather than core–RNA interactions, exists (Wang et al., 2000; Kim et al., 2003), several studies indicate that the core protein modulates HCV translation. Specifically, regions of the core protein corresponding to aa 34–44 (Zhang et al., 2002) or aa 1–20 (Li et al., 2003) are important for inhibition of HCV translation. The core protein may down- or up-regulate HCV IRES activity in a dose-dependent manner (Boni et al., 2005).

The aim of the present study was (1) to clarify the nature of interaction between the HCV core protein and the viral IRES element and (2) to gain insight into the relationship between core protein-mediated inhibition of translation and core–IRES interactions using a combination of techniques, including an in vivo reporter assay and in vitro surface plasmon resonance (SPR) analysis.

Results

Effect of the core protein-coding sequence on HCV IRES-initiated translation

Since there is conflicting data regarding the effect of the core protein or the core protein sequence on HCV IRES-directed translation (Shimoike et al., 1999; Zhang et al., 2002; Li et al., 2003; Boni et al., 2005), we sought to determine whether the RNA sequence of the core-coding region inhibits HCV IRES activity in the present experiment. A single substitution replacing A with U at nt 357 was introduced to produce a stop codon near the 5′ end of the region encoding the core protein, as previously described (Wang et al., 2000). This mutant, known as pCAGFS, produces core protein RNA with a single substitution, resulting in a core peptide, five residues in length, encoded by the N-terminal. Western blot analysis was then used to confirm that the core protein is not expressed by HepG2 cells following transfection with pCAGFS (Fig. 2C). RNA molecules transcribed in vitro from two reporter plasmids, HCVLuc and RLuc, expressing firefly luciferase (FL) controlled by the IRES of HCV genotype 1b and *Renilla* luciferase (RL) controlled by a cap-dependent mechanism, respectively, were cotransfected into cells after 48 h of transfection with pCAGFS39 or core-expressing pCAGC191 (Suzuki et al., 2001). Cell lysate samples were prepared 6 h post-reporter transfection and assayed for expression of both luciferases. As shown in Fig. 2A, the translational activity of HCV IRES was reduced in cells expressing the core protein, but not in cells transfected with pCAGFS, indicating that the HCV core protein, but not the core-coding sequence, inhibits HCV IRES-directed translation. Transfection with neither core-expressing or non-expressing constructs modulated cap-dependent translation (Fig. 2B).

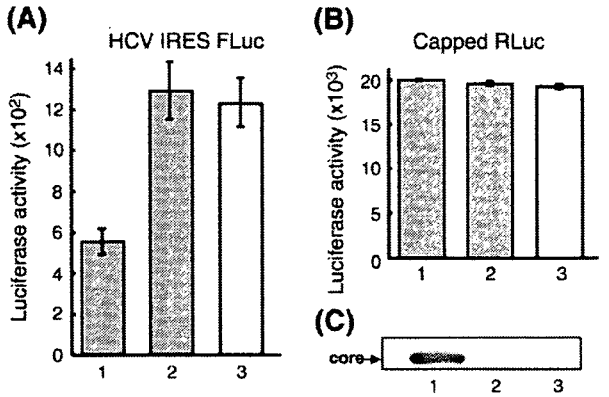

Fig. 2. Effect of the core protein-coding sequence on the translation initiated by HCV IRES. HepG2 cells transfected with pCAGC191 (lane 1), pCAGFS (lane 2), or pCAGGS (lane 3) were cotransfected with reporter RNAs of HCVLuc and the capped RLuc. The activities of both FL (A) and RL (B) were measured by a luminometer. The activities of both FL and RL were determined in at least three independent experiments, each of which conduced with triplicate samples. (C) Western blot analysis of the core protein expressed in the infected cells.

Effect of partial deletion of the HCV 5′UTR on inhibition of viral IRES-mediated translation by the core protein

In previous studies, we demonstrated that purified HCV core protein binds most efficiently and stably to the stem-loop IIId domain of the 5′UTR of HCV RNA followed by the stem-loop I domain and the region encoding nt 23–41 (Fig. 1; Tanaka et al., 2000). In addition, we revealed that the core protein expressed in HepG2 cells inhibits the IRES-dependent translation of HCV (Shimoike et al., 1999). It can be hypothesized that binding of the core protein to one or more regions of the 5′UTR might inhibit translation. To address this issue, we constructed three reporter plasmids: ΔILuc, Δ23–41Luc, and ΔIIIdLuc, with deletions of domain I (Δ1–22), nt 23–41, and domain IIId (Δ254–278) of the HCV 5′UTR, respectively, also containing the FL gene (Fig. 3A). RNA molecules transcribed from these reporter plasmids in vitro were transfected into HepG2 cells, after which luciferase activity within the cell lysate samples was analyzed. Consistent with previous reports, deletions of domain I (ΔIluc) (Luo et al., 2003; Friebe et al., 2001) or IIId (ΔIIIdLuc) (Jubin et al., 2000) profoundly impaired IRES activity, with a >95% reduction in activity (data not shown), thus demonstrating the importance of these loop structures for HCV translation. Therefore, in the following experiment, we adjusted the dose of each reporter transcript to ensure a consistent level of FL expression.

To investigate the effect of the core protein on translation mediated by wild-type or mutated HCV 5′UTR as described above, cells infected with a recombinant baculovirus carrying

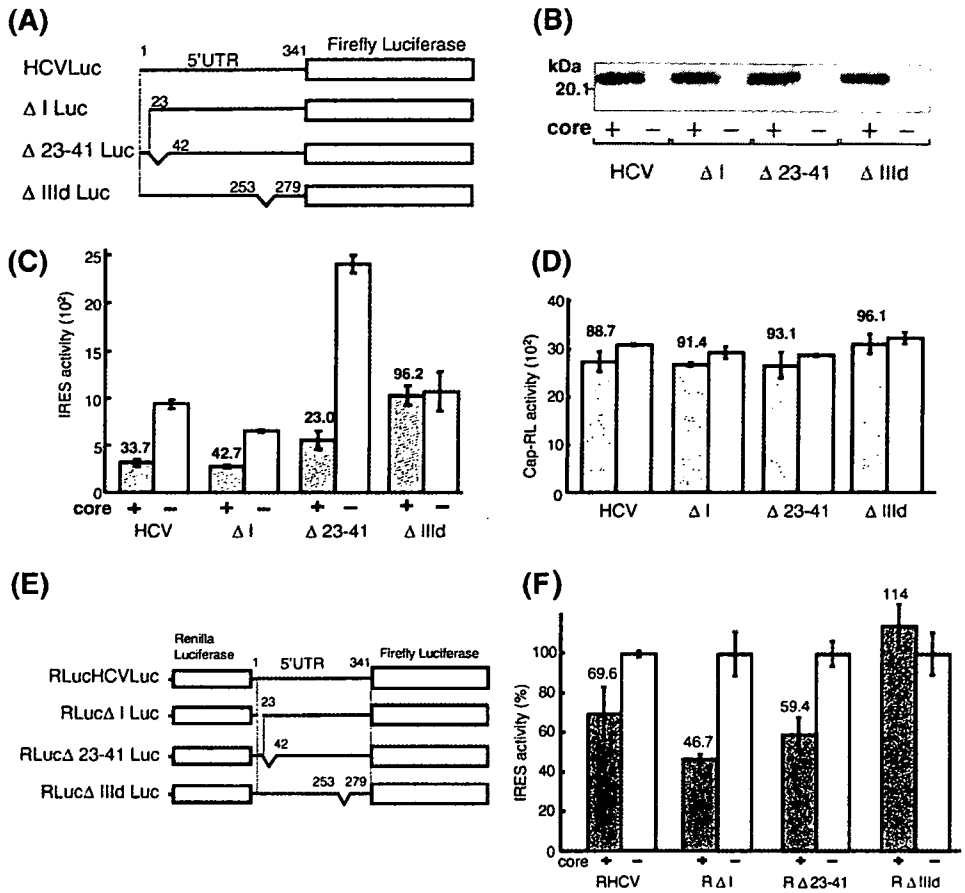

Fig. 3. Effect of deletion mutations in HCV 5′UTR on inhibition of the viral IRES-mediated translation by the core protein. HepG2 cells infected with AcCA39 or AcCAG at a multiplicity of infection of 20 were transfected with monocistronic wild-type (HCVLuc) or deletion mutants (ΔILuc, Δ23–41Luc, ΔIIIdLuc) of reporter RNAs together with the capped RLuc RNA or transfected with bicistronic wild-type (RLucHCVLuc) or deletion mutants (RLucΔILuc, RLucΔ23–41Luc, RLucΔIIIdLuc) of reporter RNAs. The activities of both FL and RL were determined in at least three independent experiments, each of which conduced with triplicate samples. Schematic representation of the monocistronic and bicistronic deletion mutants used in this study is shown in panels A and E, respectively. (B) Western blot analysis of the core protein in each cell lysate in which the luciferase activities were measured. (C) Relative luciferase activities were normalized with those of RLuc. (D) The activities of RLuc in cells cotransfected with RLuc and HCVLuc or deletion mutants are shown. (F) HCV IRES activity was determined by calculating the abundance of Fluc relative to RLuc, with that of each reporter in the absence of the core protein normalized to 100%. Mean values with standard deviations were indicated.

the entire HCV core gene (AcCA39; Shimoike et al., 1999) or an empty vector (AcCAG) were cultured for 2 days, followed by transfection with reporter transcripts, either wild-type HCVLuc (0.1 μg/well), ΔILuc (6 μg/well), Δ23–41Luc (0.2 μg/well), or ΔIIIdLuc (6 μg/well), together with capped RLuc RNA (0.08 μg/well). As indicated in Fig. 3C, expression of the core protein inhibited HCV IRES-mediated translation from ΔILuc and Δ23–41Luc, as well as from HCVLuc, by more than 50%. In contrast, inhibition of translation by the core protein was not observed in cells transfected with ΔIIIdLuc. As shown in Fig. 3D, the expression of neither the core protein nor any of the IRES-directed reporters influenced cap-directed translation. Thus, as previously demonstrated (Shimoike et al., 1999), RL activity was used as an internal control to normalize the efficiency of transfection in the following experiments (Figs. 4 and 6). Western blotting was used to confirm that core protein concentrations within the cell lysate of cells infected with AcCA39 were comparable in the presence of each of the reporter RNA molecules (Fig. 3B). We observed a similar effect of the core protein on HCV IRES activity when equal amounts (6 μg/well) of each HCVLuc, ΔILuc, Δ23–41Luc, or ΔIIIdLuc transcript were transfected (data not shown). These results eliminate the possibility that there is no translational inhibition because the core protein is destabilized in cells transfected with ΔIIIdLuc RNA. We also determined the effect of the core protein on HCV translation initiated from bicistronic reporters: RLucHCVLuc (wild-type), RLucΔILuc (deletion of domain I), RLucΔ23–41Luc (deletion of nt 23–41), and RLucΔIIIdLuc (deletion of domain IIId) (Fig. 3E). Consistent with results obtained from the monocistronic constructs, expression of the core protein showed an inhibitory effect on HCV translation mediated by RLucHCVLuc, RLucΔIluc, or RLucΔ23–41Luc, but not by RLucΔIIIdLuc (Fig. 3F). The capped RL activity from each reporter was similar and was not influenced by expression of the core protein (data not shown). These results suggest that the stem-loop IIId domain of the 5′UTR is important for inhibition of HCV translation by the core protein.

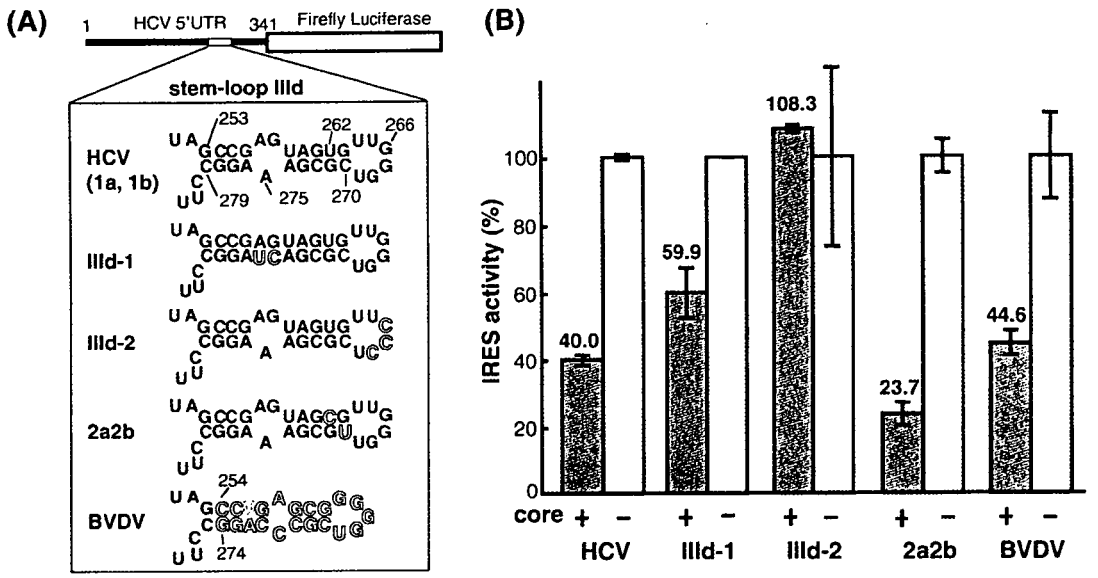

Fig. 4. Mutational analysis of the stem-loop IIId domain. (A) Schematic representation of the predicted secondary structures of the IIId domain of mutated reporters used in this study. (B) The core protein and luciferase reporters are expressed as described in the legend to Fig. 3, except reporters indicated. HCV IRES activity was determined and presented as described in the legend to Fig. 3C.

Mutational analysis of the stem-loop IIId domain

To further investigate the functional role of the stem-loop IIId domain (nt 253–279) in core protein-mediated inhibition of HCV translation, we engineered stem-loop IIId domains with the following four mutations (Fig. 4A): (1) IIId-1Luc, in which the A at nt 275 was changed to UC, thus forming a double-stranded structure instead of a bulge loop in the IIId, (2) IIId-2Luc, in which the GGG triplet (nt 266–268) was changed to a CCC triplet within the loop of stem-loop IIId, (3) 2a2bLuc, in which the U at nt 262 and the C at nt 270 were changed to C and U, respectively, thus changing the genotype to 2a/2b, and (4) BVDVLuc, in which the stem-loop IIId (nt 254–274) sequence was changed to that of bovine viral diarrhea virus (BVDV)-1. Cells that did or did not express the core protein were transfected with each of the above described reporter RNA transcripts, after which luciferase activity was measured. As shown in Fig. 4B, IIId-2Luc, containing a mutation of the GGG triplet of the apical loop, demonstrated no inhibition of HCV IRES-mediated translation by the core protein, whereas IIId-1Luc, containing a mutation within the bulge loop structure, showed only a marginally reduced inhibitory effect of the core protein. We previously demonstrated that HCV core protein binds most efficiently to (1) the stem-loop IIId domain, compared to other structural domains of the 5′UTR, and to (2) G octamer (G_8), as opposed to A_8, C_8, and U_8, using a quantitative SPR method (Tanaka et al., 2000). Thus, the results obtained here suggest that the apical loop is a critical recognition site for translational inhibition by the core protein. It is likely that the inhibitory activity of the core protein on HCV IRES-mediated translation is related to its efficiency of RNA binding.

We also observed the core protein to exert an inhibitory effect on translation directed by either 2a2bLuc or BVDVLuc, similar to that observed with wild-type HCVLuc, involving a 5′UTR sequence of genotype 1. Since the IIId domain sequence of HCVLuc is conserved among genotypes 1, 3, 4, and 5 and since that of 2a2bLuc is shared with genotype 6, it appears that inhibition of HCV translation by the core protein is independent of the viral genotype and occurs in most HCV isolates. Sequence alignment of HCV and various pestiviruses showed that, although the primary nucleotide sequence of the IIId domain exhibits considerable variability, the predicted secondary structure of the domain is highly conserved among these viruses as reviewed previously (Rijnbrand and Lemon, 1999). Furthermore, the GGG triplet followed by U at the apical loop and one bulge loop in the domain are well conserved among HCV and pestiviruses. These suggest that the nucleotide sequence of the apical loop, particularly the GGG triplet, is more important than the stem-structure sequence of the IIId domain for core protein-mediated translational inhibition.

Relationship between translational inhibition and ability of the core protein to bind to the IIId domain within the 5′UTR

To investigate the relationship between inhibition of HCV translation by the core protein and ability of the core protein to bind to IIId RNA, we prepared two biotinylated oligo RNA molecules, IIId-1 and IIId-2 (nt 251–282), containing identical mutations in the bulge and apical loops of their IIId domains as the mutated reporters IIId-1Luc and IIId-2Luc, respectively (Fig. 4A). These mutant or wild-type oligo RNA (IIId-wt) molecules were then coupled to streptavidin-coated sensor chips and allowed to bind to purified recombinant core protein. The results of subsequent SPR analysis using a BIAcore biosensor are shown in Fig. 5. The core protein was observed to bind to IIId-1 RNA as efficiently as to IIId-wt RNA,

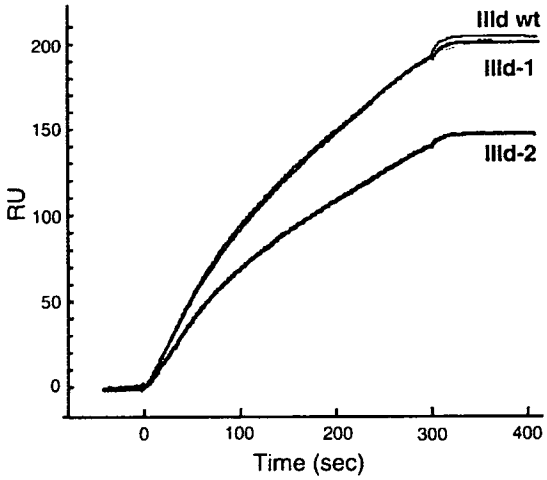

Fig. 5. Binding of the core protein to oligo RNAs corresponding to the mutated IIId domains. The real time binding between the core protein and wild-type (IIId wt) or mutants (IIId-1 and IIId-2) of the stem-loop IIId was examined. Biotinylated oligonucleotides were immobilized of the streptavidin pre-coated sensor chips followed by being exposed to 40 μl of the solution containing the core protein (4 μg/ml) with a flow rate of 8 μl/min. The sample flow was stopped, and the buffer washout began at 300 s. The amounts of immobilized synthetic oligonucleotides, IIId-wt, IIId-1, and IIId-2 were 211.0, 206.9, and 212.4 resonance units, respectively.

suggesting that RNA mutations disrupting the bulge loop structure have little or no effect on binding of the core protein. In contrast, a marked reduction in binding affinity of the core protein for mutant IIId-2 RNA was observed. As a negative control, we found that the core protein does not bind to oligo RNA corresponding to IIIe or IIIf domain (data not shown; Tanaka et al., 2000). It is likely that the apical loop sequence and/or the GGG triplet are important for RNA binding of the core protein, which is consistent with prior observations suggesting that the core protein binds to G-stretch sequence(s) with high affinity.

Combined with the data shown in Fig. 4B, the inhibitory effect of the core protein on HCV IRES activity correlates well with its ability to bind to wild-type and mutated IIId RNA. In light of the observation that the IIId domain is important for IRES activity and from suggestion that the domain IIId interacts with 40S (Otto et al., 2002; Jubin et al., 2000; Lukavsky et al., 2000; Spahn et al., 2001), the HCV core protein may inhibit viral IRES-dependent translation by preventing required interactions between RNA molecules and the 40S by binding to the IRES sequence including the apical loop of the IIId domain.

Role of basic-residue clusters within the core protein in inhibition of HCV translation

The amino-terminal portion of the core protein is able to bind to viral nucleic acids (Santolini et al., 1994). This region contains three clusters of arginine- and lysine-rich sequences (aa 5–13, 38–43, and 58–71). To investigate the role of these basic-residue clusters in inhibition of HCV translation by the core protein, we constructed a series of core mutants, in which lysine and arginine residues within one or more of the basic-residue clusters of the core protein were substituted with alanine residues, as depicted in Fig. 6A. Two days after transfection with either wild-type (pCAGC191) or core mutant (pCAGC191m1–m7) constructs, the cells were cotransfected with HCVLuc and capped-RLuc RNA. As indicated in Fig. 6B, core mutants containing alanine substitutions within one or two clusters (C191m1, m2, m3, m4, m5, and m6) retained the ability to inhibit HCV IRES-mediated translation, similar to the wild-type core protein. However, a core mutant with alanine substitutions involving all three clusters, C191m7, demonstrated little to no inhibition of translation. Expression of the core protein in each transfectant was determined by Western blotting (Fig. 6C), and none of the mutants influenced cap-dependent translation (data not shown). These results

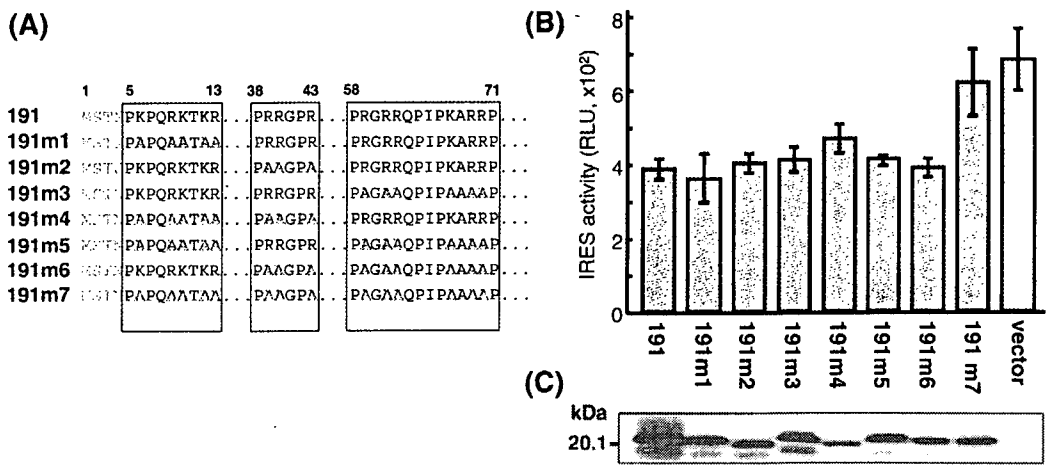

Fig. 6. A role of basic-residue clusters within the core protein in inhibition of the HCV translation. (A) Schematic representation of the mutated core proteins substituted in three basic aa clusters. Lysine or arginine residues substituted with alanine in the clusters are shown with outlined letters. (B) Two days after the transfection with either wild-type (191) or mutated (191m1–m7) core-expressing constructs, HepG2 cells were further cotransfected with HCVLuc and capped-RLuc RNAs. Relative luciferase activities (RLU) were determined as described in Materials and methods and the legend to Fig. 3. (C) The amounts of the wild-type and mutant core proteins expressed in HepG2 cells are shown by Western blotting.

suggest that all three basic-residue clusters of the core protein can mediate inhibition of HCV translation and that at least one cluster is required for inhibition.

Discussion

In this study, we investigated the mechanism by which the core protein modulates HCV IRES activity using an in vivo reporter assay and SPR technology. We demonstrated the importance of a stem-loop IIId domain, spanning nt 253–279, in core protein-mediated inhibition of HCV IRES-mediated translation. In a previous study, we demonstrated preferential binding of the core protein to domain IIId of the 5′UTR followed by domain I and a region spanning nt 23–41 (Fig. 1), upon examining 10 oligonucleotides corresponding to various structured domains of the viral 5′UTR (Tanaka et al., 2000). The core protein did not have an inhibitory effect on translation directed by mutated IRES lacking the IIId domain. However, translation initiated by IRES mutants with deletions of domain I or nt 23–41 was significantly inhibited by the core protein to a similar extent as wild-type IRES-mediated translation (Fig. 3B). Further mutational analysis was then used to determine whether specific IIId nucleotide sequences were important for inhibition of translation by the core protein. We determined that the GGG triplet (nt 266–268) within the IIId apical loop was most critical for core protein-mediated inhibition (Fig. 4B). Combined with the results of SPR analysis (Fig. 5), the data presented here suggest that inhibition of HCV IRES-directed translation by the core protein depends on the binding efficiency of the core protein for the viral IRES element.

Domain III, which is composed of six distinct regions containing stem-loop structures, forms the core of the HCV IRES and is essential for viral translation. Previous studies suggest that domain III plays a role in recruiting the 40S ribosomal subunit and eIF3 by direct interaction with stem-loops IIId/e/f and IIIb, respectively, even though the 40S subunit makes multiple interactions with the IRES and also binds to stem-loop II and the pseudoknot domain of the IRES element (Kieft et al., 2001; Kolupaeva et al., 2000; Sizova et al., 1998). Stem-loop IIId is a highly conserved region within domain III in most HCV isolates, consisting of two double-stranded helical elements separated by a 3-nt internal asymmetric loop with a 6-nt hairpin loop at the distal end of each helical region. IRES sequence deletions, including deletion of stem-loop IIId, as well as point mutations, inhibit binding of the 40S subunit and IRES function (Rijnbrand et al., 1995; Honda et al., 1996; Kieft et al., 1999). Specifically, substitution mutations of the GGG triplet within the IIId apical loop region produce significant loss of IRES activity, as well as alterations in RNA folding, indicating that the GGG triplet is a critical region for HCV translation (Kieft et al., 1999; Jubin et al., 2000). In addition, antisense 2′-*O*-methyloligonucleotides targeted to the IIId domain are known to compete with the 40S subunit for binding and to inhibit viral translation (Tallet-Lopez et al., 2003). Moreover, the secondary structure of the IIId domain is important for binding of the S9 ribosomal protein (Odreman-Macchioli et al., 2000). Consistent with these observations, we also observed that deletion of the IIId domain (ΔIIIdLuc), or a G-to-C substitution within the GGG triplet (IIId-2Luc), significantly reduced IRES activity.

Although the sequence of the IIId domain is highly conserved, sequence polymorphism of the helical region exists among the six major genotypes. With regard to nt 262 and nt 270 of the IIId domain, genotypes 1, 3, 4, and 5 of HCV encode U (nt 262) and C (nt 270), respectively. On the other hand, genotypes 2 and 6 encode C (nt 262) and U (nt 270), respectively. We observed that translation directed by the IRES sequence of genotypes 2 and 6 (2a2bLuc) was more efficient than that directed by the IRES sequence of genotypes 1, 3, 4, and 5 (HCVLuc) (Fig. 4B). Previous studies also demonstrated differences in the efficiency of IRES activity among different HCV genotypes and suggest that the 5′UTR of genotype 2(b) has the most marked IRES activity (Tsukiyama-Kohara et al., 1992; Kamoshita et al., 1997; Collier et al., 1998). Thus, sequence polymorphism involving the helical region of IIId might explain the observed variability in IRES activity when comparing the 5′UTR sequences of different HCV genotypes. Expression of the core protein inhibits HCV translation directed by 2a2bLuc to a similar or same extent as that directed by HCVLuc. This finding suggests that inhibition of viral translation by the core protein commonly occurs during the HCV life cycle and is not limited to certain genotypes. The deletion of the 5′-proximal stem-loop domain I (ΔILuc) significantly reduced IRES activity (data not shown), although the ability of the core protein to inhibit translation was retained (Fig. 3B). Published data regarding the role of domain I in inhibition of HCV translation are not consistent. Some researchers suggest that the 5′-proximal region containing domain I is not essential for HCV IRES activity (Honda et al., 1996; Kamoshita et al., 1997). However, other researchers suggest that this stem-loop element is required for optimal IRES-mediated HCV translation (Friebe et al., 2001; Fukushi et al., 1994; Luo et al., 2003). We compared HCV IRES activity mediated by monocistronic and bicistronic reporters with deletion of domain I and found that an inhibitory effect of the domain I deletion observed from the bicistronic reporter was less evident than that from the monocistronic one: the reduction in IRES activity caused by the deletion was 95% and 40% for the monocistronic and bicistronic constructs, respectively. Although similar trends were observed in the previous studies using cultured cells (Friebe et al., 2001; Luo et al., 2003; Kamoshita et al., 1997), in vitro transcription/translation studies demonstrated that the translational efficiency of the reporters deleted with domain I is higher than that of the wild-type (Honda et al., 1996; Kamoshita et al., 1997). It may be likely that differences in (1) gene constructs such as monocistronic and bicistronic reporters and (2) host cell conditions influence such inconsistent observations.

HCV core protein is highly basic, especially its N-terminal half, and it is thought to encapsulate the viral genome within a viral nucleocapsid. The RNA-binding domain of the core protein has been mapped to 75 aa residues within the N-terminal, in which three clusters of highly arginine/lysine-rich sequences are well conserved among HCV isolates (Santolini et

al., 1994). We previously observed preferential binding between the core protein and positive-stranded HCV RNA spanning the 5′UTR and part of the structural-protein coding region (nt 1–2327) (Shimoike et al., 1999). In this study, we demonstrated the importance of three basic aa residue clusters within the N-terminal region of the HCV core protein for its inhibitory effect on viral IRES activity. At least one cluster is required for inhibition of translation by the core protein. Previous studies with a series of deletion mutants suggest that aa 34–44 (Zhang et al., 2002) or aa 1–20 (Li et al., 2003) within the core protein are crucial for inhibition of translation initiated by HCV IRES. To investigate the contribution of these basic-residue-rich domains within the core protein to inhibition of viral translation, we employed substitution mutagenesis of the full-length core protein in order to reduce the occurrence of conformational changes in the core protein due to the introduction of mutations.

Although an increasing body of evidence shows involvement of the core protein in translational regulation, there are conflicting data regarding the exact mechanism by which this occurs. In contrast to studies describing direct inhibition of HCV translation by expression of the core protein (Shimoike et al., 1999; Zhang et al., 2002; Li et al., 2003), a recent report suggests that the core protein modulates HCV IRES function in a dose-dependent manner, with low amounts of the core protein producing up-regulation and greater amounts resulting in down-regulation (Boni et al., 2005). The core protein does not only inhibit translation initiated by the HCV IRES, but also cap-dependent translation and translation initiated by encephalomyocarditis virus (EMCV) IRES (Li et al., 2003). In an earlier study, neither cap- nor EMCV IRES-dependent translation were inhibited by expression of the core protein (Shimoike et al., 1999). Other studies suggest that the core protein-coding sequence, but not the core protein itself, modulates HCV IRES function, through a long-range RNA–RNA interaction (Wang et al., 2000; Kim et al., 2003). In the present experiment, however, down-regulation of HCV IRES-directed translation by the core protein-coding RNA sequences was eliminated by introducing a base-substitution mutation into the N-terminus of the core sequence in order to create a termination codon (Fig. 2). These contradictory findings might be due to different experimental conditions, such as the use of different reporter systems and host cells, as well as different levels of core protein in the assays used. To investigate the effect of the core protein on HCV IRES-dependent translation, we employed in vivo RNA transfection of monocistronic reporter constructs because HCV IRES is located at the 5′ end of the viral genome, and not internally, thus making it unnecessary to use a bicistronic reporter. Concerning bicistronic contexts, the possibility that the first cistronic sequence might influence IRES regulation directed by the second cistronic gene cannot be excluded. There is evidence to suggest that differences in translational regulation by the core protein might exist among different cell lines, including HepG2, Huh-7, and CV-1 cells (Wang et al., 2000; Li et al., 2003). We also observed differences between HepG2 and Huh-7 cells in terms of ability of the core protein to inhibit HCV IRES- and cap-dependent translation, which was not observed in Huh-7 cells (data not shown), as previously reported (Wang et al., 2000). Such cell-type specific effects might be related to differences in core protein expression since core protein expression by the recombinant baculovirus AcCA39 seems to be less abundant in Huh-7 cells, compared to HepG2 cells (data not shown). It is also possible that a cell-specific factor(s) are involved in translational regulation by the core protein. Thus, some interaction(s) between the highly ordered HCV IRES structure and/or the core protein and related host factors are likely cell-type-specific. Our previous report showed difference in the translation efficiency mediated by HCV IRES among human liver-derived cell lines, although the effect of the core protein on their translation was not determined (Aoki et al., 1998).

We performed the gel mobility shift assay to demonstrate the inhibition of the interaction between the HCV 5′UTR and the ribosome 40S subunit (40S). The complexes between purified 40S and the radiolabeled HCV 5′UTR (nt 1–330) were detected, and the amount of this band was decreased in the core protein-dose-dependent manner. In this condition, the core–5′UTR complex was competed with a non-labeled oligo RNA corresponding to IIId domain, but not with oligo RNAs of domain IV. However, the complex between the core protein and the 5′UTR was detected around the wells of the gel. To our knowledge, there has been no published data that in the gel mobility shift assay the core–5′UTR complex runs into the gel. Although these findings may support the idea that the core protein directly prevents binding of 40S to the HCV IRES, direct biochemical probing of the proposed interaction must wait for the advances in the protein chemistry of the HCV core protein.

Finally, based on the results of the present study and the existing literature, we propose a model of down-regulation of HCV translation mediated by the core protein (Fig. 7). In HCV-infected cells, the virus uncoats and releases its genomic RNA, which serves as a template for protein translation. Highly folded secondary and tertiary RNA elements in the 5′UTR function as *cis* signals for interaction with the 40S subunit and eIF3 during the initial process of HCV IRES-dependent translation. The high affinity interaction between HCV IRES and the 40S subunit is thought to be important for recruitment of the 43S particle to viral RNA, and the stem-loop IIId domain is a prerequisite for this interaction. Since the core protein binds most efficiently to the IIId domain in the HCV IRES element, it is relevant to note that the core protein may prevent an essential RNA–40S interaction by blocking the IIId domain, thereby reducing the viral translation efficiency. At an early stage of the HCV replication cycle, translation of the viral genome yields a polyprotein, which is subsequently processed to yield individual mature proteins. At a certain point, enough core protein is available to inhibit HCV translation by competing with the 40S subunit for IRES binding. Cells in which HCV translation is negatively controlled may have reduced levels of core protein due to its degradation by the ubiquitin/proteasome pathway (Suzuki et al., 2001; Moriishi et al., 2003), thereby decreasing the inhibitory effect of core protein. Thus, the core protein may

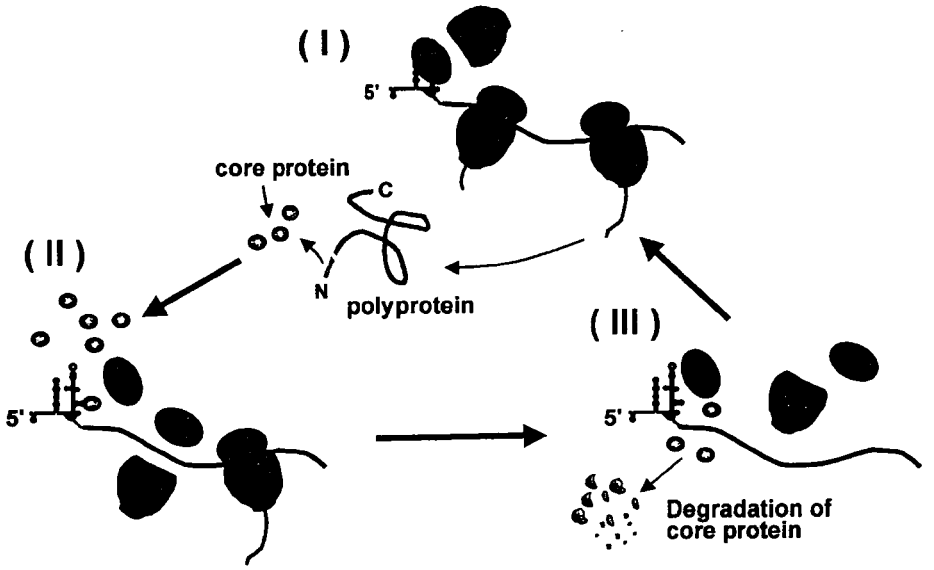

Fig. 7. Model for the regulation of HCV translation mediated by the core protein. Step 1: HCV translation is initiated through recognition of the 40S subunit and eIF3 by the IRES RNA tertiary structure. The viral polyprotein is expressed and processed into matured proteins, resulting in generation of the core protein. Step 2: The expressed core protein binds to the stem-loop IIId in the 5′UTR and inhibits the viral translation by competing with 40S subunit for binding to the IRES. Step 3: The reduced translational efficiency results in decreasing the levels of HCV proteins and replication. Degradation of the core protein through the ubiquitin/proteasome pathway may also contribute to reducing the amounts of the core protein in cells. A low concentration of the core protein possibly leads to recovery of the translational efficiency.

contribute, through its competitive interaction with the IRES IIId domain, to virus persistence by maintaining a low level of HCV replication.

Materials and methods

Plasmid construction

pT7ΔloopILuc (termed ΔILuc in this report), a 271-nt fragment containing a T7 promoter followed by nt 23–249 from the 5′ terminus of the HCV genome (clone NIHJ1; genotype 1b) (Aizaki et al., 1998), was amplified by PCR using pT7HCVLuc (HCVLuc) (Shimoike et al., 1999) as a template and primers *Hin*dIIIT7S (5′-CCCAAGCTTTAATACGACTCACTATACACTCCACCATAG-3′) and *Nhe*IAS (5′-CTAGCTAGCAGTCTCGCGCGGGG-3′). The PCR product was digested with both *Hind*III and *Nhe*I and ligated with a 5.3-kbp *Hind*III–*Nhe*I fragment of pT7HCVLuc. pT7Δ23–41Luc (Δ23–41Luc) was made using a QuickChange Site-Directed Mutagenesis Kit (Stratagene, La Jolla, CA) in order to introduce a deletion of nt 23–41 from the 5′ terminus. The primers used for PCR were 23–41S (5′-CCTAGATTGGGGGCGACCCCTGTGAGGAAC-3′) and the 23–41 AS complement (5′-GTTCCTCACAGGGGTCGCCCCCAATCAGG-3′), and pT7HCVLuc was used as a template.

pT7ΔIIIdLuc (ΔIIIdLuc) was made by digestion of pT7HCVLuc with *Nhe*I and *Stu*I, thereby generating 30-bp (corresponding to the stem-loop IIId region), 1.8-kbp, and 3.8-kbp fragments. After this, the 1.8-kbp and 3.8-kbp fragments were isolated, blunt-ended, and then ligated.

pT72a2bLuc (2a2bLuc), pT7BVDVLuc (BVDVLuc), pT7IIId-1Luc (IIId-1Luc), and pT7IIId-2Luc (IIId-2Luc) were made as follows. pT7HCVLuc was partially digested with *Stu*I. A 5.6-kbp fragment was isolated and completely digested with *Nhe*I. The resulting fragment was ligated with annealed two partially complementary oligonucleotides with the following *Nhe*I and *Stu*I sites: 5′-CTAGCCGAGTAGTGTTGGGTCGCGACTAGG-3′ and 5′-CCTAGTCGCGACCCAACACTACTCGG-3′ for IIId-1,5′-CTAGCCGAGTAGTGTTCCCTCGCGAAAGG-3′ and 5′-CCTTTCGCGAGGGAACACTACTCGG-3′ for IIId-2, 5′-CTAGCCGAGTAGCGTTGGGTTGCGAAAGG-3′ and 5′-CCTTTCGCAACCCAACGCTACTCGG-3′ for 2a2b, and 5′-CTAGCCTGAGCGGGGGTCGCCCAGG-3′ and 5′-CCTGGGCGACCCCCGCTCAGG-3′ for BVDVLuc (the underlined nucleotides were substituted for the wild type nucleotides; see Fig. 4A).

pRLucHCVLuc, pRLucΔ23–41Luc, and pRLucΔIIIdLuc: 2.6-kb fragments were amplified by PCR using pT7HCVLuc, pT7Δ23–41Luc, and pT7ΔIIIdLuc as template DNAs, respectively, and primers *Xba*I 5′endS (5′-GCTCTAGAGCCAGCCCCCGATTGGGGGCGA) and *Xba*I 3′endAS (5′-GCTCTAGAACTAGTGGATCCGGAT). The PCR products were digested with *Xba*I and ligated with a 3.3-kb *Xba*I fragment of pRL-null Vector (Promega, Madison, WI).

pRLucΔILuc: 2.6-kb fragment was amplified by PCR using pT7ΔILuc as a template DNA and primers *Xba*IloopIS (5′-GCTCTAGACACTCCACCATAGATCACCCCC) and *Xba*I 3′endAS. The PCR product was digested with *Xba*I and ligated with a 3.3-kb *Xba*I fragment of pRL-null Vector.

pCAGC191 (Suzuki et al., 2001) carries nt 329–914, containing the entire HCV coding region of the core protein of clone HCV J1 (Aizaki et al., 1998), controlled by the CAG promoter. pCAGFS contains a frame shift mutation, involving substitution of A with T at nt 357, to make a stop codon (TAA)

(refer to Fig. 1). Only the first five residues (MSTNP) of the core protein are translated from this plasmid. To create a series of mutated core-expressing constructs: pCAGC191m1, -m2, -m3, -m4, -m5, -m6, and -m7, alanine substitutions were introduced into the basic-residue clusters of the core protein by PCR mutagenesis with primers containing base alterations, as described previously (Suzuki et al., 2005). The PCR products were then cloned into pCR2.1 (Invitrogen Corp., Carlsbad, CA) and verified by DNA sequencing. Individual cDNAs were excised and inserted separately into pCAGGS. The primer sequences used in these constructions are available from the authors upon request.

Cells

A human hepatocellular carcinoma cell line, HepG2, was obtained from the American Type Culture Collection. Cells were maintained in Dulbecco's modified Eagle's medium (Nissui, Tokyo, Japan) containing 50 μg/ml of Gentamycin (Biological Industries Ltd., Israel) and supplemented with 10% fetal calf serum.

RNA preparation

The reporter plasmids were linearized by digestion with adequate restriction enzymes, and the resulting DNA fragments were used as templates for in vitro transcription. HCVLuc and a series of HCVLuc mutants were linearized by digestion with *Xho*I. pRL-null (Promega, Madison WI) was linearized by *Xba*I digestion. pRLucHCVLuc and a series of pRLucHCVLuc mutants were linearized by *Bam*HI digestion. An in vitro transcription kit, MEGAscript (Ambion, Austin, TX), was used for RNA synthesis, during which reaction mixtures containing 1 μg of DNA template and 2 μl of T7 enzyme mix were incubated at 37 °C for 2 h. For capped RNA synthesis, linearized pRL-null, pRLucHCVLuc, and a series of pRLucHCVLuc mutants were used as templates, and 2 μl of each ATP, CTP, and UTP (7.5 mM), as well as 1 μl of GTP (7.5 mM) and 1 μl of cap homologue m7G (5′) ppp (5′) G (7.5 mM; Ambion), was used. The reaction mixtures were subsequently treated twice with 2 U of DNase I at 37 °C for 20 min followed by EDTA (25 mM) and lithium chloride (3.75 M) to terminate the reaction. Capped mRNA synthesized contained 11 nucleotides at 5′UTR and no poly(A) tail.

Transfection

For DNA transfection, 100 μl of Opti-MEM (Invitrogen Corp.) and 4 μl of TransIT-LT1 reagent (Mirus Corp., WI) were mixed and incubated at room temperature for 5 min followed by the addition of 2 μg of each plasmid expressing core protein, mutant core protein, or empty vector followed by incubation for a further 15 min. For RNA transfection, synthesized reporter RNA and 2.5 μl of Tfx-20 (Promega) were mixed in 100 μl of Opti-MEM and incubated for 15 min prior to transfection. One day prior to DNA transfection, cells (2.5×10^5) were seeded into a 12-well plate. The transfection mixture described above was added to the cells in 500 μl of Opti-MEM medium after the cells were washed twice with 500 μl of Opti-MEM.

Luciferase assay

The cells infected or transfected with a recombinant baculovirus or plasmid carrying the entire HCV core gene (AcCA39 or pCAGC191) or an empty vector (AcCAG or pCAGGS) were cultured for 2 days followed by transfection with reporter RNA, either HCVLuc (0.1 μg/well), ΔILuc (6.0 μg/well), Δ23–41Luc (0.2 μg/well), ΔIIIdLuc (6.0 μg/well), IIId-1 (0.1 μg/well), IIId-2 (6.0 μg/well), 2a2bLuc (0.1 μg/well), or BVDVLuc (0.1 μg/well), along with capped RL RNA (0.08 μg/well). After 6 h of incubation, FL and RL activities were determined using the Dual-Luciferase Reporter Assay System (Promega), as previously described (Aoki et al., 1998; Shimoike et al., 1999). Luminescent signals were measured with a TR717 luminometer (Applied Biosystems Japan Ltd., Tokyo, Japan).

Western blot analysis

Expression of HCV core protein was detected by Western blotting, as previously described (Shimoike et al., 1999). Briefly, protein was transferred to a polyvinylidene difluoride (PVDF) membrane (Immobilon; Millipore, Tokyo, Japan) after separation by SDS-PAGE. After blocking, the membranes were probed with a polyclonal antibody against glutathione-*S*-transferase core (aa 1–191) fusion protein, at a 1:100 dilution.

SPR experimental procedure

To prepare the core protein, insect Tn5 cells were infected with a recombinant baculovirus Ac39. The core protein was partially purified from the cell lysate, as previously described (Tanaka et al., 2000). Interactions between the core protein and synthetic RNA oligonucleotides were examined by SPR analyses with BIAcore 2000 (Biacore K.K., Tokyo, Japan). The SPR experimental procedure was as previously described (Tanaka et al., 2000). Briefly, a biotinylated oligonucleotide spanning nt 251–282 (IIId-wt) and mutant IIId domains (IIId-1 and IIId-2) (Fig. 4A) were synthesized followed by immobilization on streptavidin pre-coated sensor chips. Forty microliters of solution containing the core protein (4 μg/ml) was injected onto the sensor chip surface at a flow rate of 8 μl/min. The sample flow was stopped, and buffer washout started at 5 min post-injection.

Acknowledgments

We are grateful to Professor J.D. Puglisi for helpful discussion. We would like to thank Drs. M. Tashiro, T. Yoneyama, H. Tani, H. Aizaki, K, and A. Cahour for helpful discussion. We are grateful to Drs. H. Tani and A. Rikimaru for constructing the recombinant baculoviruses and plasmids. We would also like to thank Ms. S. Ogawa, M. Matsuda, M.

Available online at www.sciencedirect.com
SCIENCE DIRECT
VIROLOGY
ELSEVIER
Virology 351 (2006) 381–392
www.elsevier.com/locate/yviro

Production of infectious hepatitis C virus particles in three-dimensional cultures of the cell line carrying the genome-length dicistronic viral RNA of genotype 1b

Kyoko Murakami [a], Koji Ishii [a], Yousuke Ishihara [b], Sayaka Yoshizaki [a], Keiko Tanaka [c], Yasufumi Gotoh [d,e], Hideki Aizaki [a], Michinori Kohara [f], Hiroshi Yoshioka [g], Yuichi Mori [g], Noboru Manabe [d], Ikuo Shoji [a], Tetsutaro Sata [c], Ralf Bartenschlager [h], Yoshiharu Matsuura [i], Tatsuo Miyamura [a], Tetsuro Suzuki [a,*]

[a] *Department of Virology II, National Institute of Infectious Diseases, 1-23-1 Toyama, Shinjuku-ku, Tokyo 162-8640, Japan*
[b] *Hanaichi Ultrastructure Research Institute, Okazaki, Aichi 444-0076, Japan*
[c] *Department of Pathology, National Institute of Infectious Diseases, Shinjuku, Tokyo 162-8640, Japan*
[d] *Research Unit for Animal Life Sciences, Animal Resource Science Center, The University of Tokyo, Iwama, Ibaraki 319-0206, Japan*
[e] *Unit of Anatomy and Cell Biology, Department of Animal Sciences, Kyoto University, Kyoto 606-8502, Japan*
[f] *Department of Microbiology and Cell Biology, Tokyo Metropolitan Institute of Medical Science, Bunkyo-ku, Tokyo 113-8613, Japan*
[g] *Mebiol Inc., Hiratsuka, Kanagawa 254-0075, Japan*
[h] *Department of Molecular Virology, Hygiene Institute, University Heidelberg, Im Neuenheimer Feld 345, D-69120 Heidelberg, Germany*
[i] *Department of Molecular Virology, Research Institute for Microbial Diseases, Osaka University, Suita, Osaka 565-0871, Japan*

Received 5 January 2006; returned to author with revision 23 January 2006; accepted 24 March 2006
Available online 6 May 2006

Abstract

We show that a dicistronic hepatitis C virus (HCV) genome of genotype 1b supports the production and secretion of infectious HCV particles in two independent three-dimensional (3D) culture systems, the radial-flow bioreactor and the thermoreversible gelation polymer (TGP), but not in monolayer cultures. Immunoreactive enveloped particles, which are 50–60 nm in diameter and are surrounded by membrane-like structures, are observed in the culture medium as well as at the endoplasmic reticulum membranes and in dilated cytoplasmic cisternae in spheroids of Huh-7 cells. Infection of HCV particles is neutralized by anti-E2 antibody or patient sera that interfere with E2 binding to human cells. Finally, the utility of the 3D-TGP culture system for the evaluation of antiviral drugs is shown. We conclude that the replicon-based 3D culture system allows the production of infectious HCV particles. This system is a valuable tool in studies of HCV morphogenesis in a natural host cell environment.

Keywords: Hepatitis C virus; Replication; Three-dimensional culture; Virus particle

Introduction

Infection with hepatitis C virus (HCV) currently represents a major medical and socioeconomic problem. HCV is a main causative agent of chronic hepatitis, cirrhosis, and hepatocellular carcinoma, and there are an estimated 170 million HCV carriers worldwide (Choo et al., 1989). The standard treatments for HCV infection are interferon alpha (IFN-α) in combination with ribavirin (RBV) or, more recently, a polyethylene glycol-modified form of IFN-α; however, sustained response is seen in only ~50% of treated patients (Davis et al., 2003; Manns et al., 2001). Further development of new anti-HCV drugs and vaccines has been obstructed by the lack of either a small animal model or a robust cell culture system capable of supporting viral replication and the production of infectious progeny.

HCV is a small enveloped RNA virus belonging to the family Flaviviridae and harboring a single-stranded RNA genome with

* Corresponding author. Fax: +81 3 5285 1161.
E-mail address: tesuzuki@nih.go.jp (T. Suzuki).

0042-6822/$ - see front matter © 2006 Elsevier Inc. All rights reserved.
doi:10.1016/j.virol.2006.03.038

positive polarity. A precursor polyprotein of ~3000 amino acids (aa) is encoded by a large open reading frame. This polyprotein is cleaved by cellular and viral proteases to give rise to a series of structural and nonstructural proteins (Choo et al., 1991; Grakoui et al., 1993; Hijikata et al., 1991). The establishment of selectable dicistronic HCV RNAs that are capable of autonomous replication in human hepatoma Huh-7 cells was a significant breakthrough in HCV research (Blight et al., 2000; Lohmann et al., 1999) and has provided an important tool for the study of HCV replication mechanisms and for screening antiviral drugs (Frese et al., 2001; Guo et al., 2001). This replicon system was first developed to replicate only viral subgenomic RNAs but has been further expanded to enable the replication of genome-length dicistronic RNAs (Ikeda et al., 2002; Pietschmann et al., 2002). Although the viral genome replicates and all HCV proteins are properly processed in this system, virus particle production has not yet been achieved. A number of researchers (Date et al., 2004; Kato et al., 2001, 2003) have developed an HCV genotype 2a replicon (JFH-1) that efficiently replicates in a variety of human cells. Recently, it has been demonstrated that the full-length JFH-1 genome or a chimeric genome using JFH-1 and J6, a related genotype 2a strain, produces infectious particles in cell cultures (Lindenbach et al., 2005; Wakita et al., 2005; Zhong et al., 2005). More recently, production of infectious genotype 1a virus (Hutchinson strain) using similar experimental systems has been described (Yi et al., 2006). These complete HCV culture systems produce robust levels of infectious virus and provides a powerful tool for HCV research. However, to date their applications have not been extended to constructs based on strains of genotype 1b, which is highly prevalent worldwide.

We previously demonstrated that differentiated human hepatoma FLC4 cells transfected with in vitro transcribed HCV genomic RNA can produce and secrete infectious particles in three-dimensional (3D) radial-flow bioreactor (RFB) culture (Aizaki et al., 2003). This RFB system was initially aimed to develop artificial liver tissue, and the bioreactor column consists of a vertically extended cylindrical matrix through which liquid medium flows continuously from the periphery toward the center of the reactor (Kawada et al., 1998). In RFB culture, human hepatocellular carcinoma-derived cells can grow spherically or cubically, and they retain liver functions such as albumin synthesis (Kawada et al., 1998; Matsuura et al., 1998) and drug-metabolizing activity mediated by cytochrome P450 3A4 (Iwahori et al., 2003).

In the present study, two kinds of 3D culture techniques, the RFB and the thermoreversible gelation polymer (TGP), were used for the production and secretion of infectious HCV particles by using a dicistronic HCV genome derived from genotype 1b. We also demonstrate that these 3D culture systems are useful for evaluating anti-HCV drugs.

Results

Secretion of HCV-LPs from RCYM1 carrying genome-length dicistronic HCV RNA cultured in RFB culture

We first assessed the replicative capacity of selectable genome-length HCV RNAs in FLC4 cells. However, no G418-resistant colonies were observed, indicating that FLC4 cells do not support replication of these HCV RNAs (data not shown). Therefore, subsequent experiments were carried out with a stable Huh-7 cell line, RCYM1, which supports full-length HCV RNA replication and which was developed by transfection of the cells with genome-length dicistronic RNA derived from the Con1 clone 1389neo/core-3′/NK 5.1 (genotype 1b)

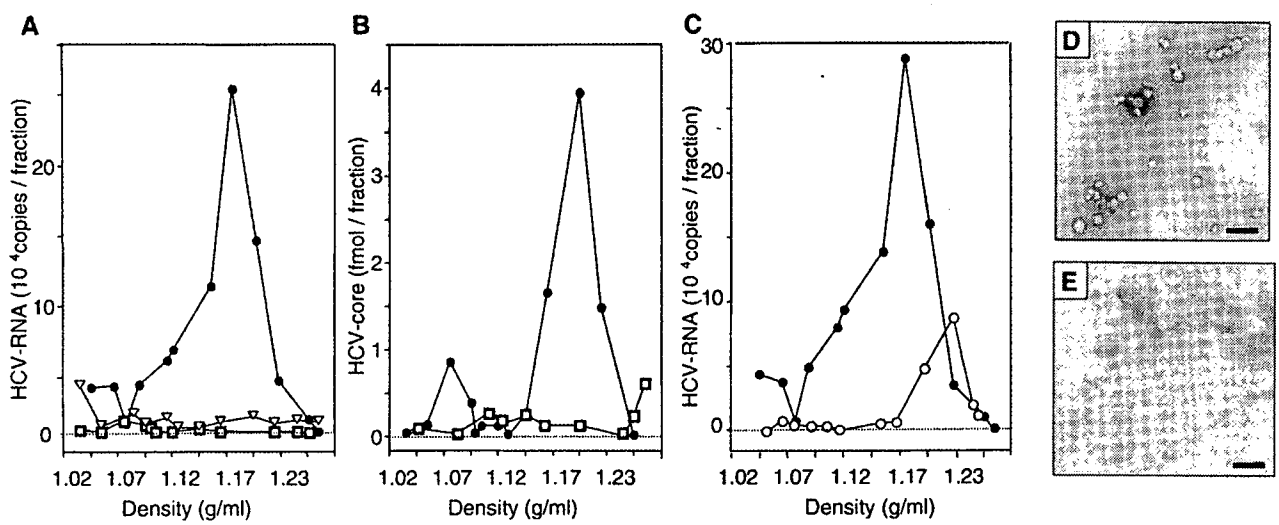

Fig. 1. Sucrose density gradient analysis of culture supernatants of RCYM1 cells. Culture media collected from radial-flow bioreactor (RFB)-cultured RCYM1 (closed circles), monolayer-cultured RCYM1 (open squares), and RFB-cultured 5–15 cells (open triangles) were fractionated as described in Materials and methods. (A) HCV RNA in each fraction was measured by real-time reverse transcriptase-polymerase chain reaction (RT-PCR). Mean values of duplicates were plotted against the density of the corresponding fraction. (B) HCV core protein in each fraction was determined by enzyme-linked immunosorbent assay (ELISA). Mean values of duplicates were plotted against the density. (C) Culture medium of RFB-cultured RCM1 cells were treated with 0.2% NP40 (open circles), followed by centrifugation in a sucrose gradient. Each fraction was tested for HCV RNA by real-time RT-PCR. (D, E) Electron microscopy analysis. Samples were prepared from the 1.18 g/ml fraction of culture media collected from RFB-cultured (D) or monolayer-cultured (E) RCYM1 cells.

(Pietschmann et al., 2002). The HCV RNA level in RCYM1 cells was approximately 5 × 10^6 copies/μg total RNA as determined by real-time reverse transcriptase-polymerase chain reaction (RT-PCR). The expression and subcellular localization of HCV protein were confirmed by Western blotting and immunofluorescence analysis (data not shown). To develop 3D RFB cultures, first we loaded RCYM1 cells onto an RFB column by flowing cell suspension, after which the cells were attached to carrier beads. Cells proliferated within the 3D matrix, and culture medium was circulated radially through the column.

In order to investigate whether HCV-like particles (HCV-LPs) were secreted from RCYM1 cells in the RFB culture system, we fractionated culture fluid collected after 5–10 days of culture by continuous 10–60% (wt/vol) sucrose density gradient centrifugation. HCV RNA and core protein were predominantly detected in the 1.15–1.20 g/ml fractions, with maximal detection in the 1.18 g/ml fraction (Figs. 1A and B). In the same experiment using 5–15 cells, in which a subgenomic HCV replicon replicates, no peak similar to that observed in RCYM1 cells corresponding to HCV RNA was detected. In both RCYM1 cells and 5–15 cells in the RFB culture system, a substantial amount of HCV RNA was detected in the 1.03–1.07 g/ml fractions (Fig. 1A). Consistent with a previous report by Pietschmann et al. (2002), these RNAs released from cells with a subgenomic replicon did not correspond to virus particles. When an equivalent number of RCYM1 cells were cultured in a monolayer culture system, limited amounts of HCV RNA and core protein were detected in the culture supernatant (Figs. 1A and B).

The mature HCV virion is thought to have a nucleocapsid and an outer envelope composed of a lipid membrane with viral envelope glycoproteins. Culture fluids were treated with NP40 in order to solubilize lipids and were then subjected to sucrose density gradient centrifugation. HCV RNA sedimented to a density of 1.22 g/ml rather than 1.18 g/ml (Fig. 1C), indicating that the density of HCV particles became higher due to de-envelopment. Transmission electron microscopy (TEM) of the 1.18 g/ml fraction, which was subjected to negative staining after concentration, revealed particle structures with diameters of 30–60 nm and a major particle size of 50 nm (Fig. 1D). No similar particle-like structures were observed in the same density fraction of the RCYM1 monolayer culture (Fig. 1E) or in the 1.23 g/ml fraction of the RCYM1-RFB culture (data not shown). These results indicate that, in the RFB system, the production and secretion of HCV-LPs is possible with a selectable dicistronic HCV genome.

Production and secretion of HCV-LPs from spheroid culture of RCYM1 cells using TGP

In the 3D RFB culture system for RCYM1 cells, extracellular secretion of HCV-LPs was observed. Based on this observation, we hypothesized that morphological changes occurring in 3D culture, such as polarity formation, promote advantageous in the assembly of viral proteins, particle formation, and extracellular secretion. To examine whether similar phenomena could be observed in other 3D culture systems, we investigated HCV-LP expression using a 3D culture system with TGP as a carrier.

TGP is a biocompatible polymer made from conjugates of polyethyleneglycol and poly-*N*-isopropylacrylamide, which is a thermoresponsive polymer composed of *N*-isopropylacrylamide and *n*-butylmethacrylate. The TGP solution possesses sol-gel transition properties; it is water soluble (sol phase) at temperatures below the transition temperature, and it is insoluble (gel phase) above it. It is possible to manipulate the transition temperatures through molecular engineering. The transition temperature for TGP in the present experiments was approximately 20 °C.

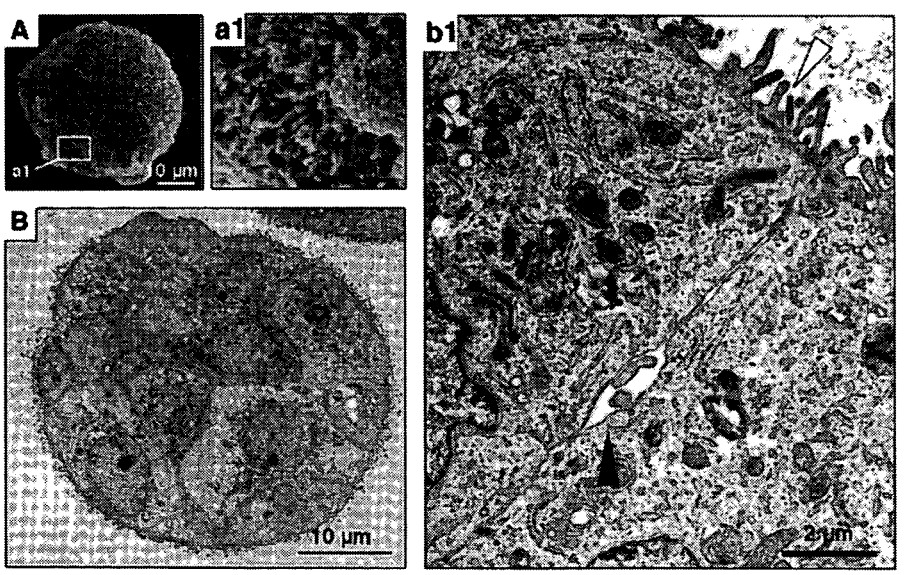

Fig. 2. Huh-7 and RCYM1 cells form spheroids in thermoreversible gelation polymer (TGP). Scanning electron microscopy (A and a1) and transmission electron microscopy (B and b1) of RCYM1 cells cultured in TGP for 8 days. Open arrowhead, microvilli; closed arrowheads, bile canaliculi-like structures.

RCYM1 cells, which were seeded into the TGP, formed three-dimensional compacted aggregates called spheroids after 3 days of culture, and numerous spheroids with diameters of approximately 1 mm were observed after 7–10 days of culture. After 8 days of culture, the spheroids were fixed and examined by scanning electron microscopy (Figs. 2A and a1) and ultrathin sections were examined by TEM (Figs. 2B and b1). Well-developed microvilli, a feature of polarized epithelium, were observed on the cell surface (Figs. 2A and a1). Bile canaliculi-like structures were also observed within intercellular spaces, and they appeared to be connected via tight junctions (Figs. 2B and b1). This cytomorphology, similar to that observed in the RFB culture (Kawada et al., 1998; Matsuura et al., 1998), correlated well with the features of mature liver tissue.

It is known that the replication of HCV replicons in Huh-7 cells depends on host cell growth. We found that the growth of RCYM1 cells in the TGP culture system was significantly slower than that of cells in monolayer culture (Fig. 3A). Accordingly, the expression of HCV proteins (Fig. 3B) in the RCYM1 spheroids was apparently lower compared to those observed in the monolayer cells. The viral RNA copy number in the spheroids was approximately one tenth of that in the monolayer culture (data not shown). The results of sucrose density gradient analysis of culture supernatant demonstrated co-sedimentation of HCV RNAs and core proteins at a density of 1.15–1.20 g/ml, with a peak at 1.18 g/ml (Figs. 3C and D). This distribution was consistent with the pattern obtained in RFB culture (Figs. 1A and B). It should be noted that in these experiments, lower cell numbers were used in the 3D cultures than in the monolayer cultures because of the slower growth of cells. As estimated from the quantitative data of the 1.15–1.20 g/ml fractions of the culture supernatants, 0.1–1 copies of HCV RNA/cell/day are produced and assembled into viral particles in the TGP-cultured RCYM1 cells.

TEM analysis of the 1.18 g/ml fraction after negative staining showed particle structures with a diameter of 50–60 nm and spike-like projections (Fig. 3E). Observation of ultrathin sections indicated a lipid bilayer-like membrane structure with a

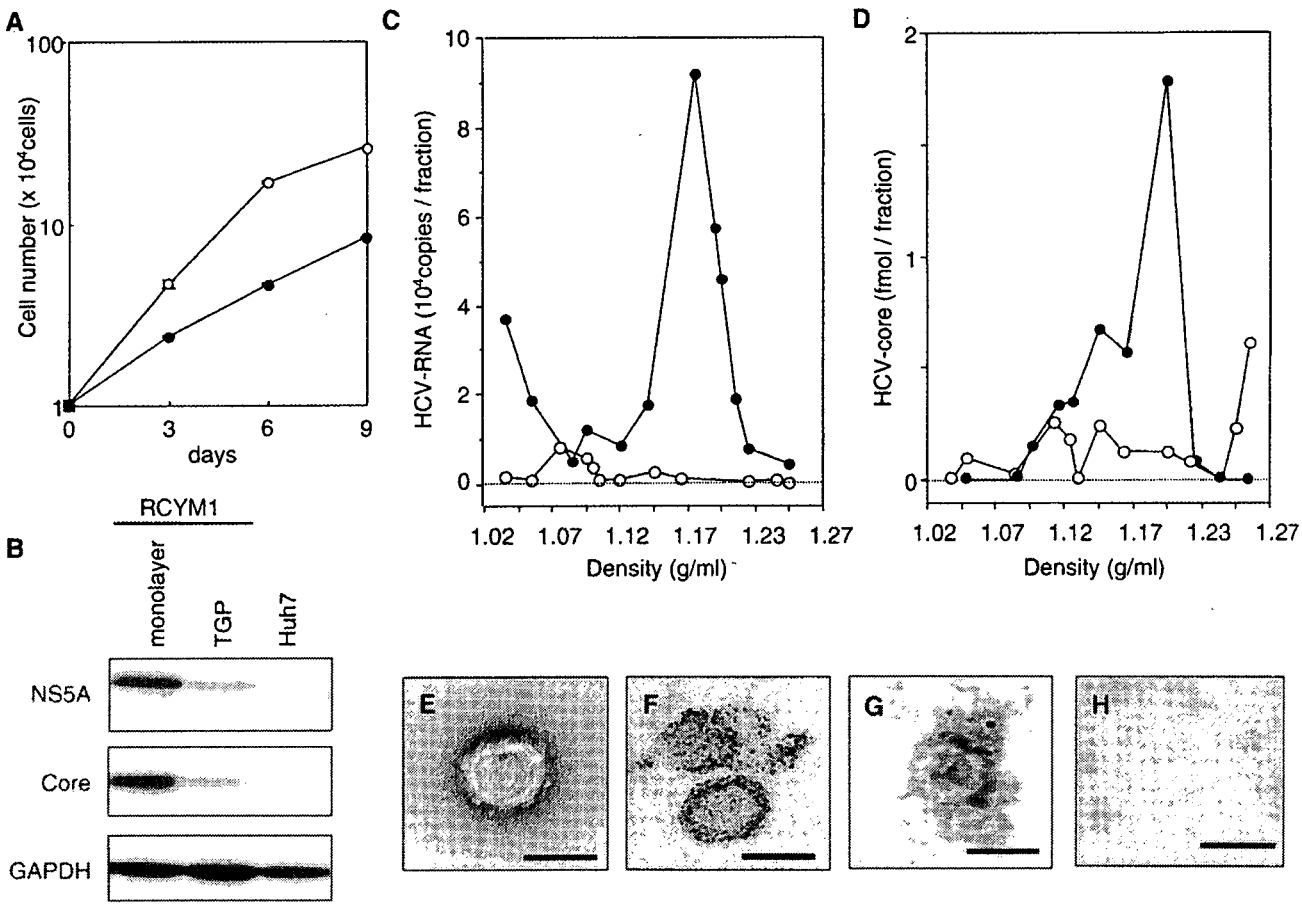

Fig. 3. Expression of HCV proteins in RCYM1 cells and secretion of viral particles in TGP culture. (A) Cell growth curves of the TGP (closed circles) and monolayer (open circles) culture of RCYM1 cells. Cells were harvested at days 0, 3, 6, and 9 postinoculation and cell numbers were determined. (B) Western blotting of HCV core and NS5A proteins in RCYM1 cells and control Huh-7 cells. (C, D) Sucrose density gradient analysis of culture supernatants of RCYM1 cells. The culture supernatants were fractionated as described in Materials and methods. HCV RNA (C) and core protein (D) in each fraction were determined by ELISA and real-time RT-PCR, respectively. Representative data from three independent experiments are shown. Closed circles, TGP culture; open circles, monolayer culture. (E–H) Electron microscopy of HCV-like particles (HCV-LPs) in the supernatants of TGP-cultured RCYM1 cells. (E) Negative staining of HCV-LPs in the 1.18 g/ml density fraction. There was no spherical structure in 1.05 g/ml density fraction, as shown in panel H. (F) Ultrathin section of HCV-LPs. Precipitated HCV-LP samples were prepared from the 1.18 g/ml fraction as described in Materials and methods. (G) Immunogold labeling of HCV-LPs with an anti-E2 antibody in the 1.18 g/ml density fraction. Gold particles, 5 nm; scale bars, 50 nm.

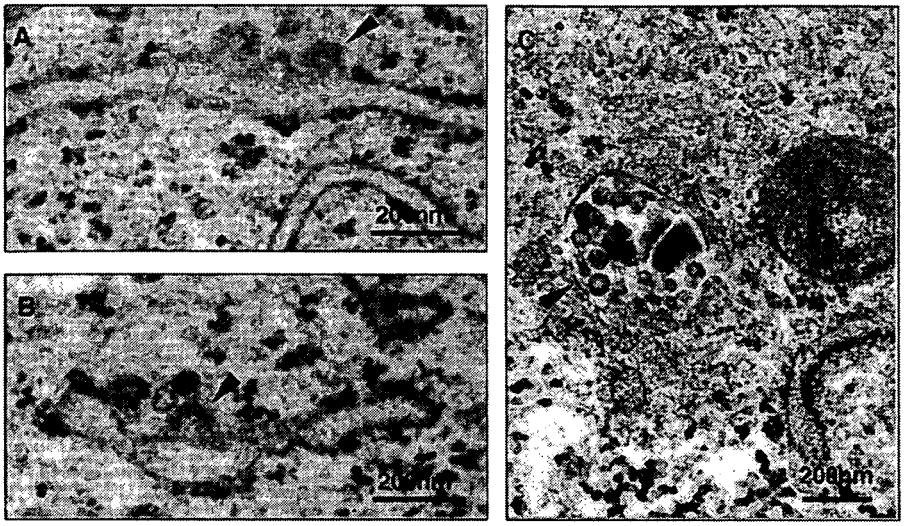

Fig. 4. Electron microscopy of ultrathin sections of RCYM1 cells grown in TGP. HCV-LPs in TGP-cultured RCYM1 cells. Spherical virus-like particles 50–60 nm in diameter (arrowheads) were observed at the ER membranes (A, B) and in the cytoplasmic vesicles (C).

width of approximately 5 nm (Fig. 3F). Immunoelectron microscopic study using anti-E2 antibody revealed HCV envelope protein(s) on the particle surface (Fig. 3G). Substantial amounts of HCV RNA were detected in the 1.03–1.05 g/ml fractions of the supernatant (Fig. 3C); however, HCV-LP structures were not observed in these fractions (Fig. 3H). These results were consistent with those from the RFB system, as shown above. The efficacy of 3D cell culture systems in virion formation was thus demonstrated in both the RFB and TGP culture systems using human liver-derived cells.

Ultrastructural localization of HCV-LPs in TGP-cultured spheroids of RCYM1 cells

We next determined the intracellular localization of HCV-LPs produced in RCYM1-TGP culture at the ultrastructural level by electron microscopic (EM) analysis of ultrathin sections. Spherical particles having membrane-like structures with short surface projections (diameter, 50–60 nm) were observed primarily at the endoplasmic reticulum (ER) membrane (Fig. 4A) as well as in the dilated cisternae of the ER (Fig. 4B). In vesicles, these virus-like particles were frequently associated with amorphous materials (Fig. 4C). In a previous study, Shimizu et al. (1996) report that virus-like particles with similar morphology and size were observed in human B cells infected with HCV. No similar particle-like structures were observed in RCYM1 cells in monolayer culture or in subgenomic replicon 5–15 in cells in TGP culture (data not shown).

In order to determine whether the virus-like particles observed by conventional TEM in the present experiment were HCV-LPs, we conducted immunoelectron microscopic analysis with anti-core antibody and anti-E1 antibody. Double-labeling experiments showed that the virus-like particles associated with the ER membrane exhibited immunoreactivity for both HCV proteins, and that the E1 protein surrounded the core proteins (Fig. 5A). To the best of our knowledge, this is the first report to clearly demonstrate that the viral envelope protein surrounds the core protein in HCV particle formation. As a negative control, thin sections prepared from subgenomic RNA containing 5–15 cells were stained with these antibodies and were found to exhibit negligible levels of background immunostaining (data not shown).

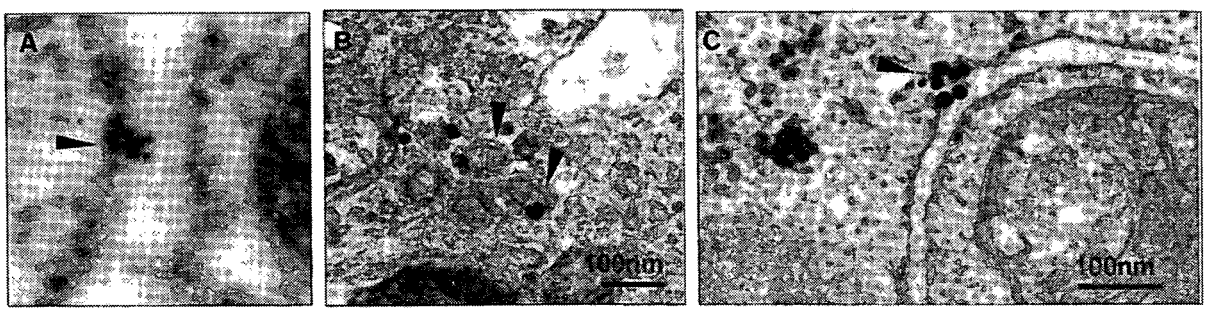

Fig. 5. Immunoelectron microscopy of ultrathin sections of TGP-cultured RCYM1 cells. (A) Double immunostaining with anti-E1 and anti-core monoclonal antibodies. Core protein-specific gold particles (10 nm in diameter) and E1 protein-specific gold particles (5 nm in diameter) formed rosettes on the surface of the ER membrane. (B and C) Silver-intensified immunogold staining with anti-core (B) and anti-E1 (C) antibodies. The second antibody conjugated with gold particles 1.4 nm in diameter was applied, followed by enlargement of the particles by the silver enhancement reagent. Arrowheads indicate virus-like particles reacting with anti-core and/or anti-E1 antibodies.

It is generally difficult to visualize intracellular microstructures and perform antigenic protein localizations using immunogold electron microscopy due to the low resolution and contrast of micrographs. In order to overcome this difficulty, we applied a silver-intensified immunogold labeling method in our experiment (Figs. 5B and C). Using this method, antigen-reactive immunogold particles approximately 20 nm in diameter were observed. Specific immunolabeling of core and E1 protein was detected in the ER or on the ER membranes. Intense immunopositive reactions were also seen on the virus-like particles observed in cytoplasmic vesicles and on ER membranes; however, no such immunolabeling was observed when normal mouse serum was used as a first antibody (data not shown). These results confirm the ultrastructural observations of conventional TEM and suggest that the formation of HCV particles is achieved by budding of the putative core particles at the ER membrane.

Infectivity of HCV-LPs depends on E2 glycoprotein

To determine whether HCV-LPs released from RCYM1 cells cultured in the TGP system are infectious, we inoculated naive Huh-7.5.1 cells (Zhong et al., 2005), which are HCV-negative Huh-7.5 (Blight et al., 2002)-derived cells, with a culture supernatant of RCYM1 spheroids. HCV RNAs in the cells at days 0, 1, 2, 3, and 7 postinoculation were determined by real-time RT-PCR. Fig. 6A shows the kinetics of HCV RNA after the inoculation of HCV-LPs. HCV RNA levels in the infected Huh-7.5.1 cells fluctuated at the indicated times, reaching 10^3–10^4 copies/μg of cellular RNA at days 1–7. Immunofluorescence staining 4 days postinoculation revealed that approximately 1% of cells were positive for NS5A protein (Fig. 6B). In contrast, no NS5A-positive cells were detected when the cell supernatant sample obtained from 5 to 15 cell cultured in TGP was used to inoculate Huh-7.5.1 cells (data not shown). These results suggest that HCV-LPs released from TGP-cultured RCYM1 cells are infectious.

To further determine whether viral envelope proteins mediate infection by HCV-LPs, we preincubated HCV-LPs with the anti-E2 monoclonal antibody AP33, which demonstrates potent neutralization of infectivity against HCV pseudoparticles carrying E1 and E2 proteins representative of the major genotypes 1 through 6 (Owsianka et al., 2005), or with patient sera with high titers of HCV neutralization of binding (NOB) antibodies (Ishii et al., 1998), or with anti-FLAG antibody (Fig. 6C). NOB antibodies have the ability to neutralize the binding of E2 protein to human cells (Rosa et al., 1996), and NOB3 and NOB4 were sera obtained from patients who recovered naturally from chronic hepatitis C (Ishii et al., 1998). Intracellular HCV RNA levels were decreased by 43%, 28%,

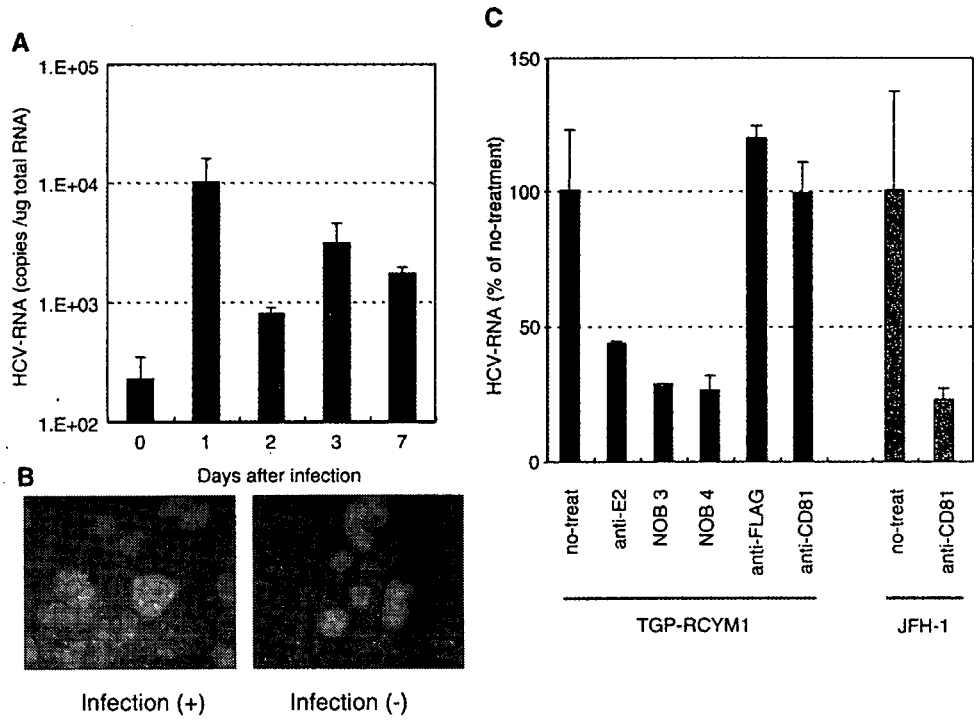

Fig. 6. Infectivity of HCV-LPs secreted from TGP-cultured RCYM1 cells and neutralization of the infection. (A) Kinetics of HCV RNA after the infection of HCV-LPs. Huh-7.5.1 cells were infected with HCV-LPs and harvested at days 0, 1, 2, 3, and 7. HCV RNAs in the cells were determined by real-time RT-PCR. (B) Huh-7.5.1 cells infected with HCV-LPs (upper panel) or without infection (lower panel) were cultured for 4 days, followed by immunostaining with anti-NS5A antibody. Nuclei were counterstained with 4′,6-diamidino-2-phenylindole (DAPI). (C) Huh-7.5.1 cells were infected with HCV-LPs after pretreatment with anti-E2 antibody AP33, neutralization of binding (NOB) antibodies, or anti-FLAG antibody. Anti-human CD81 antibody was preincubated with Huh-7.5.1 cells prior to the infection. Huh-7.5.1 cells were infected with HCV-LPs derived from TGP-cultured RCYM1cells or JFH1 virus and incubated for 4 days; HCV RNAs in the cells were determined by real-time RT-PCR. The inhibition rate is given as the percentage of the no-treatment controls. Average values with standard deviations in triplicate samples are shown. Closed bars, HCV-LPs secreted from TGP-cultured RCYM1 cells; shaded bars, JFH1 virus.

and 26% in the presence of AP33, NOB3, and NOB4, respectively. No reduction of viral RNA in infected cells was observed following treatment with anti-FLAG antibody. Thus, the present results suggest that viral envelope proteins play a crucial role in the infectivity of HCV-LPs produced by RCYM1 cells cultured in TGP. We further tested anti-CD81 antibody for inhibition of the virus infection in our system. As shown in Fig. 6C, pretreatment of the cells with the anti-CD81 antibody resulted in no inhibition of the intracellular HCV RNA level in the infected cells. In contrast, under the same condition of treatment, the antibody efficiently inhibited the infection of JFH-1 virus, which was produced from the HCV JFH-1 molecular clone as previously described (Wakita et al., 2005; Zhong et al., 2005), suggesting that CD81 has no or little, if any, need for the infection of HCV produced in our system.

Potential use of the TGP culture system for HCV production and evaluation of antiviral agents

In a recent report, Lindenbach et al. (2005) found that a cell culture system supporting complete replication of an HCV genotype 2a clone is useful for the evaluation of antiviral drugs. However, to date this complete HCV culture system has not been extended to genotype 1b, which is more frequently detected in patients with hepatitis C and is the most difficult to treat.

We show here the potential utility of the TGP culture of RCYM1 cells for evaluating anti-HCV drugs (Fig. 7). Intracellular HCV RNA levels in TGP-cultured RCYM1 cell spheroids were reduced by 90% after 3 days of culture with 100 IU/ml of IFN-α (Fig. 7A). Likewise, the extracellular HCV particle level, which was calculated using the HCV RNA copy number of the 1.18 g/ml supernatant fraction, was reduced by 89% by IFN-α treatment (Fig. 7B). Moreover, the production of HCV particles was inhibited by treatment with 100 μM RBV to the same degree (85%) as intracellular HCV RNA (Fig. 7B). The level of HCV RNA detected in the 1.04 g/ml fraction of the culture supernatant of the untreated group was approximately one fourteenth of that in the 1.18 g/ml fraction, and the level increased with the addition of IFN-α or RBV (Fig. 7B). Although the mechanism underlying this increase is unknown, a similar phenomenon was observed when several highly cytotoxic agents were evaluated using TGP-RCYM1 cultures (data not shown). It is therefore likely that some cellular proteins associated with HCV RNA are released into the culture supernatant as a result of cell death caused by the moderate cytotoxic effects of IFN and RBV.

Collectively, these results demonstrate that the HCV production model based on TGP culture is useful for evaluating HCV particle production and the inhibitory effects of anti-HCV drugs.

Discussion

In the present report, we describe that HCV-LPs are assembled and released from Huh-7 cells harboring a dicistronic genome-length Con1 HCV RNA in two independent 3D culture systems. The HCV-LPs closely resemble virus-like particles detected in the sera of patients with hepatitis C in terms of both particle size and morphology. The HCV-LPs released into the culture supernatant have a buoyant density of approximately 1.18 g/ml, which is much higher than that of putative HCV particles isolated from patient sera reported previously (Andre et al., 2002; Kanto et al., 1994; Nakajima et al., 1996; Trestard et al., 1998) and slightly higher than the average density of virus particles produced with the JFH-1 isolate (Wakita et al., 2005). One possible explanation is that the HCV particles are highly bound to lipids and low-density lipoproteins in patient sera. In agreement with a recent report (Wakita et al., 2005), our EM examination demonstrated that HCV-LPs are 50–60 nm in diameter and are composed of core-like particles with a diameter of approximately 30 nm that are surrounded by ER-derived E1/

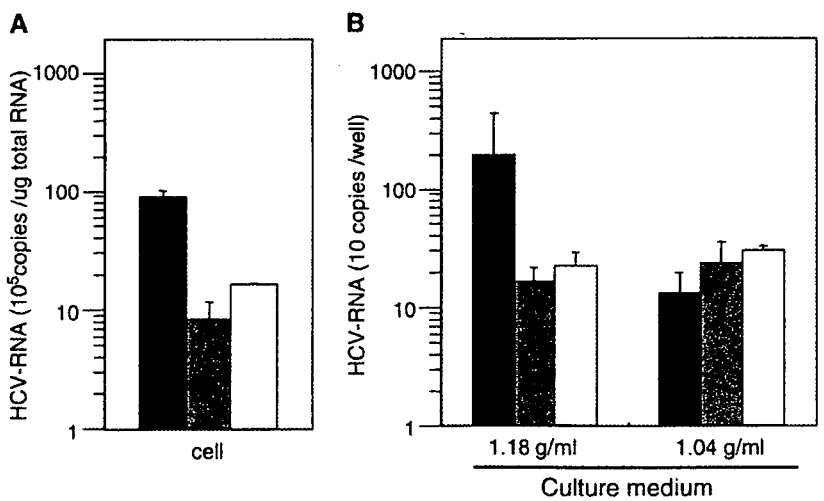

Fig. 7. Inhibition of HCV-LP production by IFN and RBV. TGP-cultured RCYM1 cells were treated with 100 IU/ml IFN-α or 100 μM RBV, and HCV RNAs in the cells (A) and in the culture media (B) were then determined. Culture media from each sample were fractionated by sucrose gradient centrifugation and HCV-LP positive (1.18 g/ml) and negative (1.04 g/ml) fractions were assayed. Average values with standard deviations in triplicate samples are shown. Closed bars, no-treatment control; shaded bars, IFN-α; open bars, RBV.

E2 proteins. These particles are observed at the ER membranes and in dilated cisternae of the ER, suggesting that the interaction of the ER membrane containing HCV envelope proteins with the viral core protein drives the budding process of HCV particles into the ER lumen.

Although studies on the ultrastructure and morphogenesis of HCV-LPs have been conducted using recombinant viral vectors carrying HCV structural protein genes (Baumert et al., 1998; Blanchard et al., 2002, 2003), the present study provides the first visual evidence of assembly and budding of HCV particles in a heterologous expression system in which a full-length viral genome is replicating and the viral particles are secreted into the culture medium. We also demonstrated that the HCV-LPs produced in our 3D culture system are infectious and that their infection is prevented by the monoclonal antibody AP33 directed against E2 (Owsianka et al., 2005) as well as by NOB antibodies (Ishii et al., 1998), which are sera of patients naturally resolving from chronic hepatitis C and exhibiting neutralizing activity. This result is consistent with the recent demonstration that E2 is required for the infectivity of JFH-1 virus (Wakita et al., 2005). It has been shown that CD81 interacts with E2 (Pileri et al., 1998) and that anti-CD81 antibodies or a soluble CD81 fragment block the infection of Huh-7 cells with either pseudotyped retroviral particles, JFH-1 virus or J6/JFH1 chimera (Lindenbach et al., 2005; Netski et al., 2005; Wakita et al., 2005; Zhong et al., 2005). Inconsistent with these studies, however, we found that anti-CD81 antibody did not inhibit the virus infection in our system. Although CD81 is considered to represent an important component in HCV entry, there are several other candidate cellular receptors for HCV (Bartosch and Cosset, 2006) and a study has demonstrated that in vitro binding of HCV to hepatoma cell lines was not inhibited by the anti-CD81 antibody (Sasaki et al., 2003).

In a previous report (Aizaki et al., 2003), we describe the production and release of infectious HCV particles from a human hepatocellular carcinoma-derived cell line, FLC4, using RFB culture in two experiments: inoculation of cells with infectious plasma from an HCV carrier and transfection of cells with viral RNA transcribed from the full-length cDNA of genotype 1a, which is known to infect chimpanzees. These findings prompted us to use the RFB system to create a culture model of HCV production based on genome-length dicistronic viral RNA, which has not been found to produce viral particles in standard monolayer cultures. As expected, HCV-LPs were produced and secreted into the medium during RFB culture of RCYM1 cells, whereas virus production was not observed in the conventional monolayer culture of RCYM1 cells. The presence of the viral envelope protein(s) on the HCV-LPs obtained in the RFB culture was strongly suggested from their density analysis with and without NP40 treatment.

We also created another 3D environment supportive of RCYM1 culture using TGP, a chemically synthesized biocompatible polymer which has a sol-gel transition temperature, thus enabling us to culture cells three-dimensionally in the gel phase at 37 °C and to harvest them in the sol phase at 4 °C, without enzyme digestion (Yoshioka et al., 1994). In contrast to other matrix gels made from conventional natural polymers and developed for 3D culture, including matrigel (Kleinman et al., 1986), collagen gel (Lawler et al., 1983), and soft agar, TGP has several advantages that allow us to investigate the functional characteristics of epithelial cells, their tissue-like morphology, and their potential clinical applications. The use of 3D culture materials other than TGP requires treatment with appropriate digestive enzymes or heating to collect cells grown as spheroids from the culture media, and the matrices may damage the cultured cells to some extent. Thus, it is difficult to keep the viable cells in a functionally and structurally intact. In addition, because matrigel and collagen gel are made from animal or tumor tissue, the possibility that certain pathogens or unidentified factors might influence cell function cannot be excluded. In the present study, we found that Huh-7 and RCYM1 cells formed an organized structure of spheroids after 7–10 days of culture in TGP, and that HCV-LPs were assembled and released from RCYM1 spheroids, as observed in RFB culture. It can be ruled out that HCV-LPs, RNA, and core protein detected in the TGP culture supernatant are released by damaged and/or broken cells because neither digestive enzymes nor heating is used in the culture procedures and no cell damage has been observed in the cultures.

It remains to be clarified why HCV particles were produced from Huh-7 cells harboring the genome-length dicistronic HCV RNA more efficiently in the 3D cultures than in the monolayer cultures. However, this might be related to the fact that directional protein transport in hepatocytes occurs more readily in 3D culture. EM examination demonstrated that, in the RFB and TGP culture systems, human hepatoma cells, such as Huh-7, FLC4, and FLC5 cells, self-assemble into spheroids with possible polarized morphology in which microvilli develop on the cell surface and channels resembling bile canaliculi and junction structures are created in the intercellular spaces (Aizaki et al., 2003; Iwahori et al., 2003). In contrast, human hepatoma cells adhere when grown on a plastic surface, growing as a flat monolayer without exhibiting the characteristics of polarized epithelium. In general, the interaction of viruses with polarized epithelia in the host is one of the key steps in the viral life cycle. A variety of viruses, especially enveloped viruses, mature and bud from distinct membrane domains of the host cells (Compans, 1995; Garoff et al., 1998; Schmitt and Lamb, 2004; Takimoto and Portner, 2004). For example, several respiratory viruses, such as influenza virus, parainfluenza virus, rhinovirus, and respiratory syncytial virus, are released preferentially from the apical surface. Conversely, other viruses egress from the basolateral membrane; these include vesicular stomatitis virus, Semliki Forest virus, vaccinia virus, and certain retroviruses. Thus, it is likely that more organized intracellular trafficking pathways exist in the 3D culture of Huh-7-derived cells, thereby driving the assembly and release of HCV.

The efficient production of HCV in 3D cultures could also be due to the reduction of HCV RNA replication and/or translation in 3D cultures as compared to those in monolayer cultures. RNA replication and/or translation of HCV replicons in Huh-7 cells are highly dependent on host cell growth (Pietschmann et al., 2001). In the present study, we found that the slow growth of spheroids resulted in reduced expression of HCV protein and

viral RNA in 3D-cultured RCYM1 cells compared to that in monolayer cultures containing similar cell numbers. The doubling time of cells grown in TGP or RFB culture was approximately twice that observed in monolayer culture. Although it is possible that amino acid substitutions of culture-adaptive mutations contribute to interference with virus production, another possibility might be that in cases of certain HCV clones, higher expression of the viral proteins leads to their misfolding, thereby precluding the formation of virus particles.

Complete cell culture systems for HCV have recently been developed (Lindenbach et al., 2005; Wakita et al., 2005; Zhong et al., 2005) using a genotype 2a isolate, JFH-1, obtained from a Japanese patient with fulminant hepatitis (Date et al., 2004; Kato et al., 2001, 2003). Unlike many other HCV isolates, JFH-1-based subgenomic replicons do not require culture-adaptive mutations for efficient RNA replication (Kato et al., 2003). Transfection of Huh-7 cells with the full-length JFH-1 genome or a chimeric genome using JFH-1 and J6 results in the efficient production of infectious HCV (Lindenbach et al., 2005; Wakita et al., 2005; Zhong et al., 2005). This newly established HCV culture system is undoubtedly useful for a variety of HCV studies; however, these systems rely on the JFH-1 replicase (NS3 to 5B) and little is known about the reasons that this particular isolate permits efficient HCV production. Virus yield in the 3D systems presented here is significantly lower than that in systems based on JFH-1; it seems that 0.1–1 copies of HCV RNA/cell/day are generated and assembled into viral particles. The ratio of viral RNA to the core protein in these fractions is approximately 10^5 RNA copies/1 fmol of the core. Although only moderate production of HCV particles is observed in 3D culture of RCYM1 cells, this is the first study to demonstrate the production of infectious HCV particles derived from genotype 1b, which is highly prevalent worldwide and is thought to present a higher risk of developing hepatocellular carcinoma and/or cirrhosis than infections with other HCV types (Bruno et al., 1997; Silini et al., 1996). The findings of the present study may also suggest that an extremely high efficiency of viral replication, such as that observed in the case of JFH-1 isolate, is not needed to produce HCV particles in 3D cultures of Huh-7 cells. Heller et al. (2005) report HCV virion production in a culture transfected with the genomic cDNA of genotype 1b; however, the infectivity of the virus particles remains to be determined. More recently, it was shown that chimeric HCV containing structural proteins of genotypes 1a, 1b, or 3a was produced from fusion of the core to the p7 or NS2 region with downstream nonstructural regions of JFH1 clone, but that intergenotypic chimeras frequently yielded lower titers of infectious HCV compared to JFH1 or J6/JFH1 chimera (Pietschmann et al., personal communication). The 3D culture system described in the present study might be a helpful method of increasing the efficiency of assembly and release of intergenotypic chimeric HCV.

In summary, we found that the expression of dicistronic genome-length Con1 HCV RNA of genotype 1b in 3D-cultured Huh-7 cells yields infectious virus particles, and we demonstrated the usefulness for producing HCV particles of two 3D culture systems based on RFB and TGP, in which human hepatoma cells can assemble into spheroids with potentially polarized morphology. HCV morphogenesis occurs in a complex cellular environment in which host factors may either enhance or reduce the assembly and budding process. The culture system described here will allow us to further study viral morphogenesis and the biophysical properties of HCV particles, and it provides a new tool for the future development of anti-HCV drugs.

Materials and methods

Cell lines bearing dicistronic HCV RNAs

To generate a stable cell line harboring genome-length dicistronic HCV RNA, we electroporated 10^7 Huh-7 cells with 50 μg of the RNA transcribed from a plasmid pFKI389neo/core-3′/NK5.1 (Pietschmann et al., 2002). The cells were maintained in Dulbecco's modified Eagle's medium with 10% fetal bovine serum and 0.5 mg/ml G418 (Promega). After stringent selection for 3 weeks, a fast-growing clone was isolated and designated as RCYM1. A Huh-7-derived cell line, 5–15, harboring a subgenomic replicon (Lohmann et al., 1999) was also used.

3D cell cultures

The RFB system (Able, Japan) was manipulated as described previously (Aizaki et al., 2003) with minor modifications. Briefly, the RFB column, being filled with 4 ml of porous carrier beads made from polyvinyl alcohol, seeded with 1×10^7 of RCYM1 or 5–15 cells. The cells were cultured in ASF104 medium (Ajinomoto, Japan) supplemented with 4 g/l of D-glucose, 2% fetal calf serum, and 0.5 mg/ml of G418 (Promega). TGP (Mebiol Gel MB-10; Mebiol, Japan) was supplied as a lyophilized form and its aqueous solution was prepared before use as previously described (Hishikawa et al., 2004; Nagaya et al., 2004; Yoshioka et al., 1994). Briefly, TGP in a flask was dissolved in 10 ml of the culture medium and was maintained at 4 °C overnight. To prepare HCV particles, we suspended 5×10^6 cells of RCYM1 in 10 ml of TGP solution and aliquots were poured into a multi-well plate. Upon warming to 37 °C, the TGP solution quickly turned into a gel form, and 3 volumes of the culture medium were added to cover the gel. To recover spheroid cells and the culture supernatant after cultivation, we subjected the cultured plate to a temperature of 4 °C for 10 min to dissolve the gel. In order to separate spheroid cells from the culture medium, we subsequently centrifuged the TGP culture diluted with the overlaid culture medium at 1000×*g* for 5 min.

Sucrose density gradient centrifugation

The culture medium collected from the RFB or TGP was centrifuged at 8000 × *g* for 50 min to remove all cellular debris, after which the supernatant was centrifuged at 25,000 rpm at 4 °C for 4 h with an SW28 rotor (Beckman). The precipitant was suspended in 1 ml of TNE buffer [10 mM Tris–HCl (pH 7.8), 1 mM EDTA, 100 mM NaCl] and was then layered on top of continuous 10–60% (wt/vol) sucrose gradient in TNE buffer,